NASA CONTRACTOR REPORT • NASA CR-66114

RIGIDIZATION OF A 1.52-METER DIAMETER INFLATABLE SOLAR CONCENTRATOR IN VACUUM WITH ASSOCIATED MATERIAL STUDIES AND FABRICATION TECHNIQUES

Prepared by
GOODYEAR AEROSPACE CORPORATION
AKRON, OHIO

for LANGLEY RESEACH CENTER

NATIONAL AERONAUTICS AND SPACE ADMINISTRATION • DECEMBER 1966

NASA CR-66114
(GAC Report No. GER-12679)

RIGIDIZATION OF A 1.52 METER DIAMETER INFLATABLE SOLAR CONCENTRATOR IN VACUUM WITH ASSOCIATED MATERIAL STUDIES AND FABRICATION TECHNIQUES

N. Jouriles
Dr. C. E. Welling
J. C. Kryah

Prepared under Contract NAS 1-5513, Control No. L-5959
by Goodyear Aerospace Corporation
Akron, Ohio

for

NATIONAL AERONAUTICS & SPACE ADMINISTRATION

ABSTRACT

Paraboloidal solar concentrator development work was carried out. Precoat foam was used as the rigidizing material for inflatable film type mirrors. 1.52 meter diameter units were rigidized in a vacuum chamber utilizing radiant heat as the heat source for initiation of the foaming reaction. The foam had been previously applied in sheet form to the back of a commercial aluminized polyimide film parabolic membrane.

A torus-type backup structure was subsequently attached for mounting in ground test equipment. Relatively good quality mirrors were the result of this development program.

AUTHOR

CONTENTS

FIGURES

FIGURES (CONTINUED)

TABLES

RIGIDIZATION OF A 1.52 METER DIAMETER INFLATABLE SOLAR CONCENTRATOR IN VACUUM WITH ASSOCIATED MATERIAL STUDIES AND FABRICATION TECHNIQUES

By N. Jouriles, Dr. C. E. Welling and J. C. Kryah

SUMMARY

This report covers a 9-month effort to improve fabrication techniques and demonstrate the utility of a precoat foam for rigidizing a 1.52 meter solar concentrator in vacuum.

A commercial aluminized polyimide film, 2.54×10^{-5} m thick, was tailored to a paraboloidal configuration and seamed with an adhesive specially chosen and evaluated for use on this solar concentrator foam rigidized in a vacuum. The membrane solar concentrator was attached to a test fixture where it was pressurized, aligned, and measured for contour. The precoat rigidizing material was made up into thin sheets and cut into patterns to fit the paraboloidal contour. The precoat sheet stock was applied to the inflated membrane solar concentrator, A heating unit, which was part of the test fixture, was placed in position, and thermocouples were imbedded in the precoat material. The vacuum chamber (NASA-Langley 18.29 m sphere) was evacuated to less than 0.13 Newton/m^2 (10^{-3} mm Hg). Heat was applied at such a rate that a temperature rise of 7°K per minute was achieved. After approximately 10 minutes the foaming action began. About 3 minutes later, the mirror was completely foamed and the foam began to set. Application of heat was continued several minutes longer to aid in curing the foam. The heat was then gradually reduced. Cool-down time from peak temperature to room temperature was approximately 40 minutes. Temperature was monitored by use of 34 thermocouples, and was controlled by means of a rheostat. After cool-down the vacuum was released. Upon return to atmospheric pressure, all thermocouples were removed and a ring torus was applied as a backup structure. The torus was bonded to the solar concentrator by means of a relatively flexible urethane foam system. The solar concentrator was then cut away from the pressure envelope, and trimmed to 1.52 meter diameter.

INTRODUCTION

A predistributed plastic foamable material for rigidizing inflatable solar energy concentrators was developed on a small scale under NASA Contract NAS 1-3301. The program herein reported, initiated by Langley Research Center (LRC), was a continuation of research and development on rigidized inflatable solar energy concentrators. The objective of this program was to improve the fabrication techniques and demonstrate the utility of the foam by fabricating a solar concentrator of a size sufficient to provide meaningful data for qualitative analysis. To accomplish this objective, research and development in critical problem areas were required, and a solar concentrator that incorporated all developed process refinements was fabricated. The program was divided into three tasks:

Task 1. Rigidization Material Studies

All effort in this area was to be restricted to the standard 394-91 precoat formulation that was described in NASA Technical Report CR-235, Development of a Predistributed Azide Base Polyurethane Foam for Rigidization of Solar Concentrators in Space. Research was to consist of an exploration of the problems associated with the synthesis, purity, handling, and storage of the required amounts of azide. In addition, the synthesis of the prepolymer was to be scaled up to produce sufficient quantities to fabricate 1.52-meter diameter solar concentrators. Application of the precoat formula to the membrane was to be studied using the sheet stock approach. Bonding of a precoat rigidized structure to a stiffening backup structure was to be studied to determine the optimum approach.

Task 2. Seam Development

Seaming of the polyimide film was to be studied to determine the best adhesive to be used. Such factors as membrane pressure, exothermic heat of precoat activation, peel strength and heat dwell time were to be considered. The goals in this area were to develop seams that would have adequate strength and suitable optical properties.

Task 3. Fabrication of a 1.52-Meter Diameter Solar Concentrator

A 1.52-meter diameter, 60-degree rim angle solar concentrator was to be fabricated using the standard 394-91 precoat formulation and polyimide film and incorporating the processes developed under Tasks 1 and 2. The concentrator was to be

rigidized in a vacuum at a starting pressure not greater than 0.13 N/m^2 of mercury. After foaming and curing in a vacuum, a stiffening backup structure was to be added to make the concentrator suitable for testing in a 1-g environment with surface winds of not more than 5.14 m/s. The backup structure was to have a torus at the rim with provisions for a solar tracker mounting at 120-degree intervals. Design goals for the concentrator were to include a specular reflectance of 0.80 and surface slope errors of 1/2 degree or less over 95 percent of the area. The concentrator was to be foam rigidized at the Langley 18.29 m sphere vacuum facility.

DISCUSSION OF DEVELOPMENT EFFORT

General

The development work carried out was in three broad categories including (1) rigidization material studies, (2) seam development, and (3) fabrication of 1.52-meter diameter solar concentrators. The fabrication task was conducted in the vacuum sphere at Langley Research Center, although the material was prepared, and a special fixture designed and built at GAC.

The three basic tasks are discussed individually in this section of the report, and closely follow chronologically the sequence followed in the program.

Material Studies

Azide studies. - In order to facilitate use of Structure X azide (4, 4' - diphenyl methane diacyl azide)

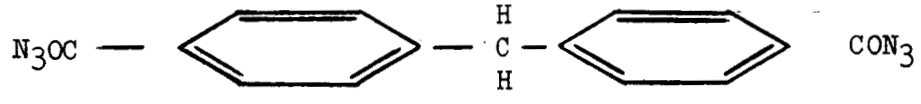

in preparing precoat material, some investigations were made concerning methods of analysis for purity, the presence of impurities in as-synthesized material, and methods for purification and general behavior of the azide in handling and storage. The results of these somewhat limited investigations are outlined here.

Azide purification: Recrystallization techniques were found that produce purified Structure X azide that is free of detectable impurities when using thin layer chromatography examination. Melting points were increased from about 356 - 356.5°K to about 358 - 359°K. The key feature

in the techniques is the use of somewhat polar solvents which make a decolorizing charcoal treatment (for impurity removal) more effective. Such solvents as mixed methylene chloride and ethanol are effective; acetone is more difficult to use in recrystallizing and, perhaps, less effective. The solution and decolorizing steps were conducted at room temperature, and the recrystallization at reduced temperatures. Attempts were made to limit the time in which samples were in solution or exposed to solvents. These handling procedures were used to ensure a minimum of azide decomposition during the purification. In view of the very slow rate of hydrolysis of solid azide under water, anhydrous solvents were not employed. All purified samples were stored at 260.9 to 266.4°K. Purification resulted in removing color and has yielded a product in fine, needle-crystal form. Findings with respect to recrystallization were transmitted to the azide supplier and led to higher purity of the product.

Efforts to purify Structure X azide by vacuum sublimation were not fruitful. The vapor pressure of the material was too low within the temperature range in which it is certainly stable. To sublime at higher temperatures might defeat our purpose by producing decomposition products that might sublime more readily. This work further establishes that one of the original goals in the molecular design of an azide structure has been achieved. The goal was to realize negligible volatility of the subject azide under pre-foaming and foaming conditions in the space environment.

A second operable method for purification of Structure X azide would be desirable in principle, partially because a single method may not remove all types of impurities effectively. However, time and funding limitations precluded further exploratory research. At this time it appears that column chromatography would be the most promising new approach in any further work, since it could be operated at temperatures at which the azide is quite stable.

Impurity and Azide Assessment: Findings are summarized in the following paragraphs. In one or two respects the findings were unexpected.

Thin layer chromatography (TLC) has proved useful in separating impurities from samples of Structure X azide. Funding has not permitted work on identification of impurities, but it is established that impurities either originally present or produced by slow decomposition during extended refrigerated storage of dry azide may be separated and detected. The TLC procedures used are essentially qualitative.

The general parameters of the TLC method employed are:

(1) Glass plates coated with silica gel containing 10 percent gypsum binder are employed. Applied coatings are generally 1000 μm thick. The coated plates are activated at 383°K.

(2) Samples are spotted at the bottom of the plates in quantities of 10 to 50 nm^3 of 2 percent concentration solutions of azide materials in acetone. Thus, the actual weight of azide taken for a single spot chromatogram is 0.2 to 1.0 mg.

(3) Elution is with a benzene-acetone solution at room temperature for 30 minutes. In this time the most rapidly moving material, Structure X, moves approximately four inches.

(4) All components eluted (azide and impurities) are colorless, non-fluorescing, and not readily developed into colored materials. Therefore a fluorescing aerosol overspray is applied. On subsequent inspection by illumination with short-wave ultraviolet light (black light) the areas containing eluted components appear as black spots on a generally fluorescent background. That is, components present quench fluorescence of the overspray.

Several conclusions may be drawn from TLC work. The first is that TLC detects small amounts of impurities in azide samples, probably below the one percent level. This is done under mild analytical conditions that do not degrade azide. A second conclusion drawn is that laboratory treatment with charcoal and recrystallization reduces impurities to undetectable levels. By the same type of postsynthesis processing, our supplier now produces azide with an impurity level below detection.

The third conclusion is that two types of impurities are seen in azide stored under refrigeration for approximately 15 months. The one type migrates very little, if at all, in elution and is presumably either of rather high molecular weight or a poor solute in the eluting solution. The second type of impurity elutes, or migrates upward on the plate, at about one half the speed of the azide. No conclusion can be reached as to the proportion of impurities that developed in the storage period. Some impurity was originally present as evidenced by the slight yellow discoloration of the material as received. The same two types of impurities are developed if a pure (recrystallized) azide sample is held as a dilute solution in acetone for two to three days at room temperature.

Figures 1, 2, and 3 illustrate the results obtained with TLC. The photographs of the TLC plates are made with ultraviolet illumination of the plates; the photographic negatives respond to the induced fluorescence.

Various samples of freshly purified (recrystallized) Structure X azide (Samples 2, 3, and 4) and of 15-month stored azide (Sample 1) were supplied for study to the spectrophotometry group of the Research Analytical Services Department of the Goodyear Tire and Rubber Co. The samples were known to differ in melting point, presence or absence of impurities detectable by TLC, and in visible color. The major effort was placed on infrared inspections since this might afford clues as to chemical

SAMPLE A: 15 MONTH OLD MATERIAL PURIFIED BY RECRYSTALLIZATION. APPLIED 50 nm^3 OF 2 PERCENT SOLUTION IN ACETONE.

SAMPLE B: NEW MATERIAL AS RECEIVED FROM THE SUPPLIER. APPLIED 50 nm^3 OF 2 PERCENT SOLUTION IN ACETONE.

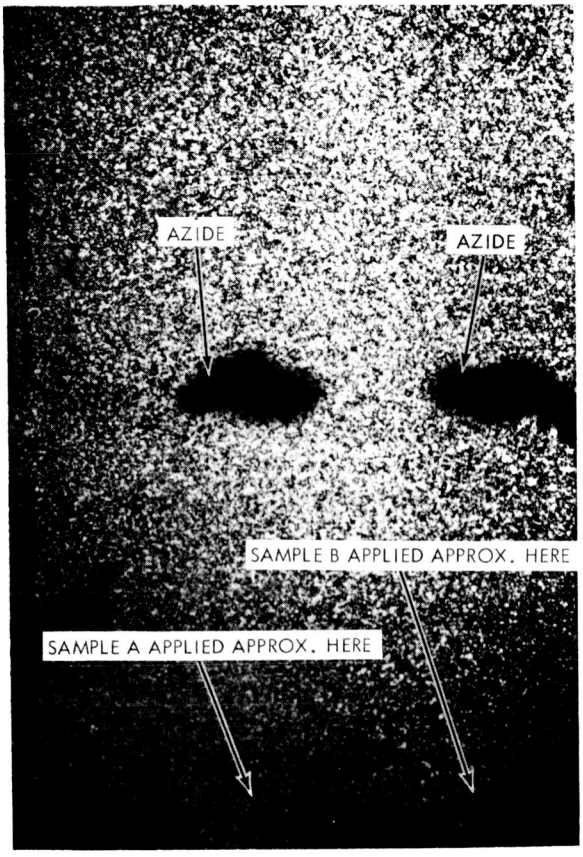

Figure 1. - Thin layer chromatography of Structure X samples (no impurities detected).

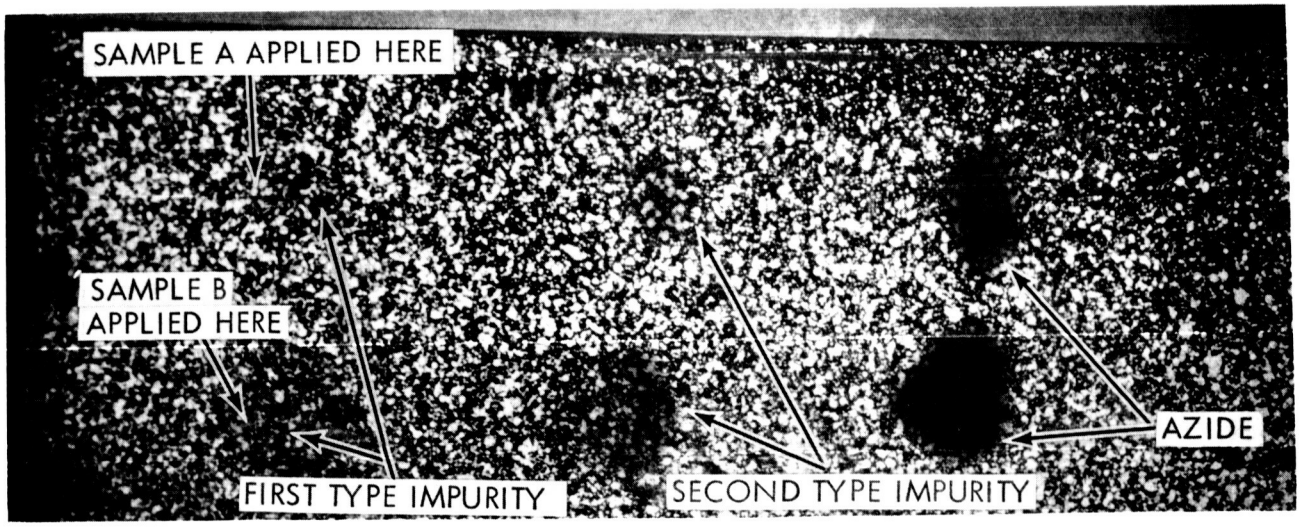

SAMPLE A: APPLIED 10 nm^3 OF 2 PERCENT ACETONE SOLUTION.
SAMPLE B: APPLIED 50 nm^3 OF 2 PERCENT ACETONE SOLUTION.

Figure 2. - Thin layer chromatography of Structure X azide after 15 months refrigerated storage (two types of impurities detected).

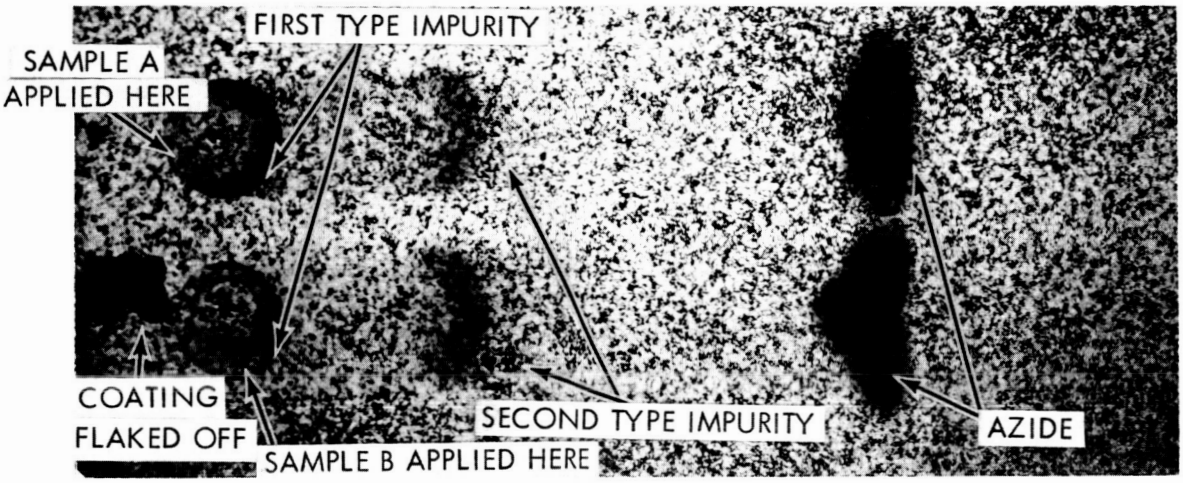

SAMPLE A: 50 nm^3 OF AGED SOLUTION
SAMPLE B: DUPLICATE OF A

Figure 3. - Thin layer chromatography of pure Structure X azide (suffered partial decomposition standing in acetone solution at 297°K for 2 - 3 days).

structure of impurities. The conclusions drawn from the infrared work employing carbon tetrachloride and chloroform as solvents are discussed in the following paragraphs.

The impurities known to be present in Sample 1 do not yield recognizable characteristic absorptions. This may be due to their absorptions being masked by bands of the major component (the azide), to the low concentration of the impurities, or conceivably to the impurities being poorly soluble in the solvents employed. This point is illustrated in Figure 4. Samples 1 (impure) and 2 (pure) and the solvent are scanned sequentially with a high-resolution grating spectrophotometer and recorded on this chart. The scans of Samples 1 and 2 are indistinguishable.

Measurements with a sodium chloride prism spectrophotometer were made of the absorption band peaking at 2138 cm^{-1}. This is characteristic of the azide group in Structure X for all four samples. The absorptivities were calculated therefrom and the values are shown below for sample solutions in chloroform at 12 kg/m^3 concentration.

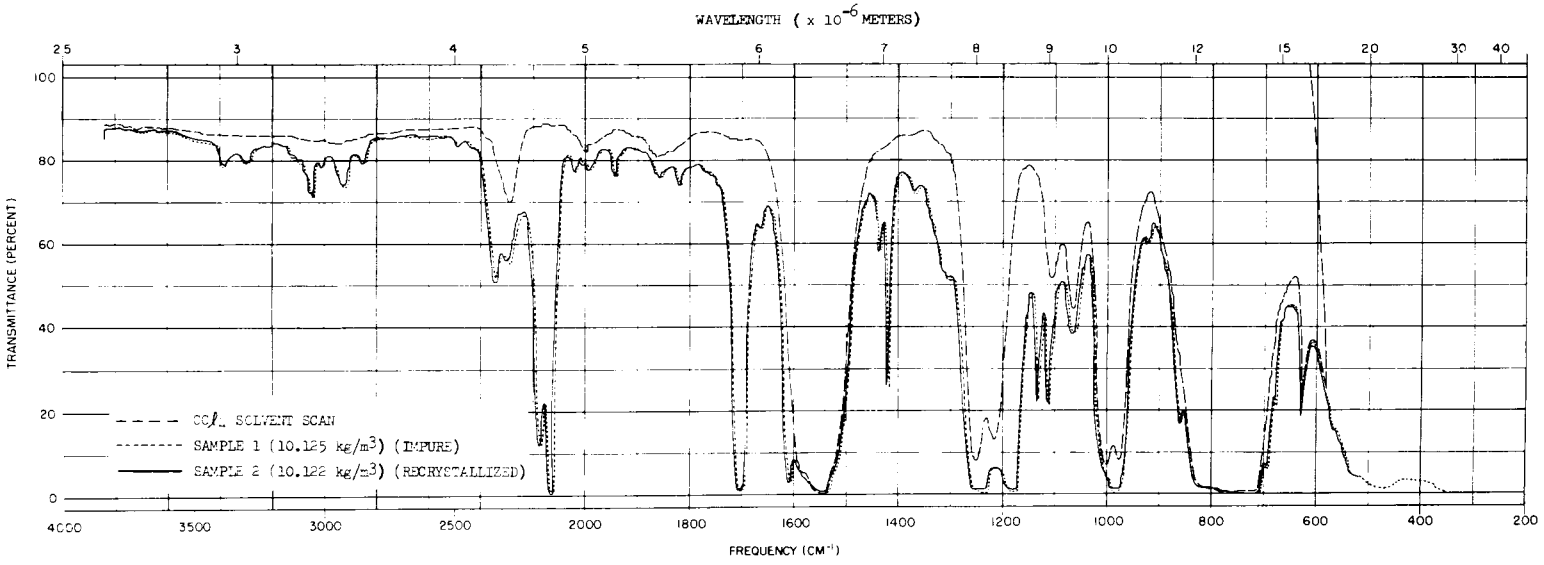

Figure 4. - Infrared absorption spectra of two samples of Structure X azide in CCl_4 solution and of solvent.

Sample	Absorptivity at 2138 cm^{-1}* ($m^3/g-m$)
1 (impure)	0.287
2 (pure)	0.289
3 (pure)	0.294
4 (pure)	0.289

Since there is no other evidence that Sample 3 is of greater purity than 2 or 4 and since other absorptivity measurements with the P.E. 521 reverse the order of Samples 3 and 4, it is difficult to conclude that the small differences in the numerical values are meaningful. However, from the scatter in the above absorptivities, the conclusion may be drawn that the concentration per gram of azide function in Sample 1 is, within the limits of error of measurement, equal to that of the purified samples. In view of the TLC results, we then tentatively conclude that Samples 2, 3, and 4 are probably above 99 percent pure and Sample 1 has 97 percent or better purity.

It should be mentioned that no attempt was made to recover impurities in concentrated form from the recrystallization work for infrared examination. This would have been highly desirable from the spectroscopist's viewpoint, but promised to be a time-consuming effort.

A limited investigation with ultraviolet spectrophotometry was made of the Structure X samples described above. The results are readily interpretable and are summarized in the following paragraphs.

At low concentrations of azide in carbon tetrachloride solvent, such as 0.01 kg/m^3, an absorption band peaking at 264 nm is formed which is taken to be characteristic of Structure X. Two sets of measurements of absorptivities at 264 nm were made with the following results.

Sample	Absorptivity at 264 nm* ($m^3/g-m$)	
1 (impure)	15.2	14.6
2 (pure)	16.1	15.1
3 (pure)	15.3	15.4
4 (pure)	14.7	15.1

As in the infrared work, it appears from the direct assay standpoint that the purity of Sample 1 is equivalent to that of 2, 3, and 4 within the scatter of the measurements, which appears to be about ±3 percent.

At a high concentration of azide in solvent (10 kg sample/m^3 CCl_4) all samples are essentially opaque below 320 nm. However, Sample 1 (impure) exhibits a distinct, well developed shoulder on the absorption curve in the 330-375 nm region and lesser absorption

*Concentration is in g/m^3 and cell length in meters.

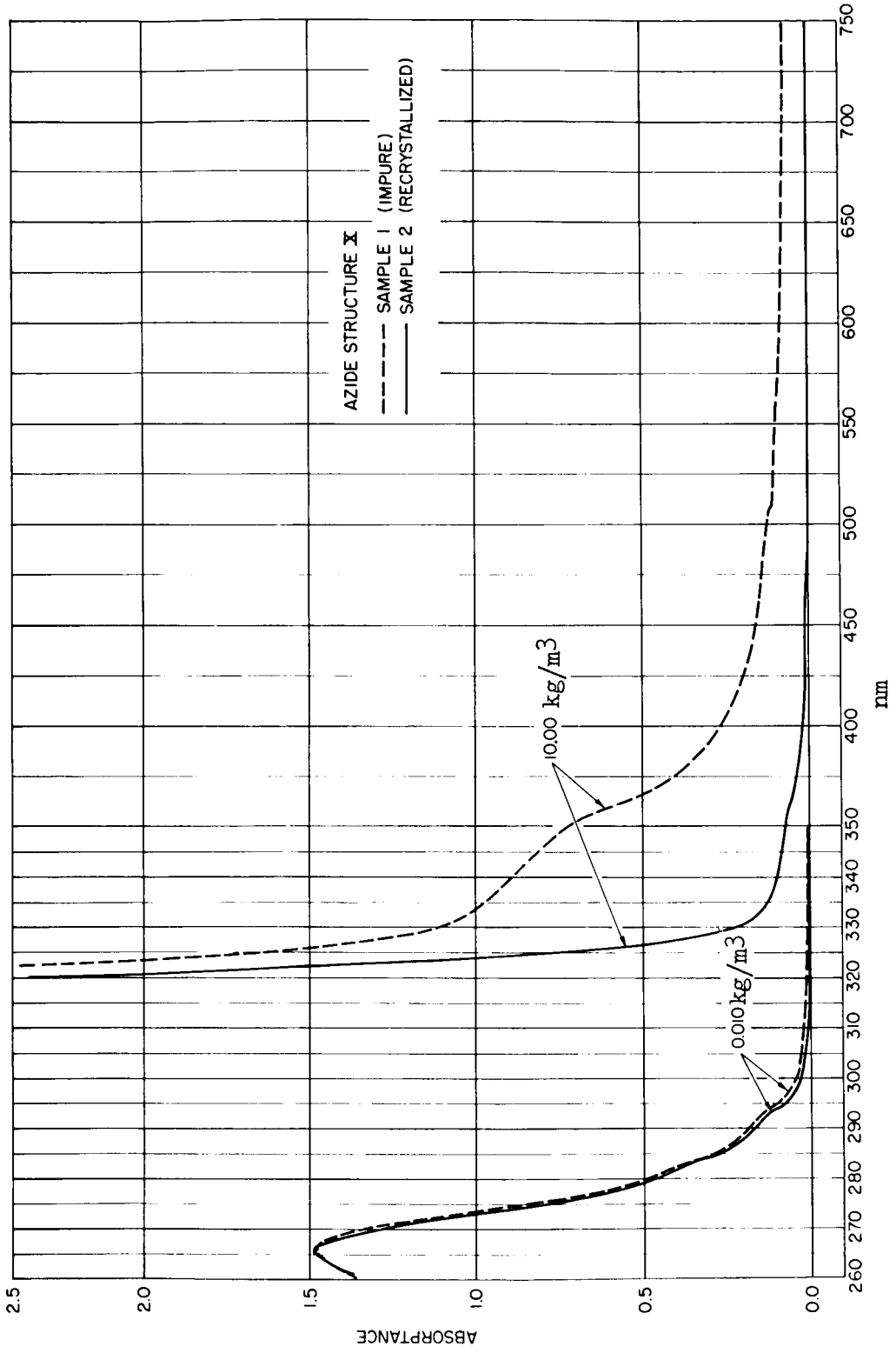

Figure 5. - Ultraviolet absorption spectra of two samples of Structure X azide in CCl_4 solution.

trailing across the entire range to 750 nm. The purified samples do not exhibit this, so the effect may be ascribed to impurities in Sample 1. The differences in absorption between impure and pure samples should have immediate utility as a criterion for purity. The present completed investigation does not establish whether the extraneous absorption shown by Sample 1 is brought about by only one or by both types of impurities found by TLC to be present in Sample 1.

The ultraviolet absorption spectra at low and high concentrations for Samples 1 and 2, obtained by successive scans recorded on the same chart of a spectrophotometer, are reproduced in Figure 5.

Storage and handling of azide: Storage of crystalline Structure X azide at temperatures in the range of 260.9 to 286°K seems satisfactory for minimizing degradation in view of our overall experience.

It was found that Structure X suffers practically no hydrolysis on 20-day standing under water at room temperature. It was also found to be easy to filter Structure X out of a water slurry and to recover free-flowing material of unaltered melting point by room temperature drying. These findings indicate the possibility of employing water slurries in some situations to eliminate shock and heat sensitivity of the azide.

Prepolymer studies.

Prepolymer production: An 0.02 m^3 reactor located in facilities of the Goodyear Tire and Rubber Company was employed for preparation of two prepolymer batches. A photograph of the steam-jacketed reactor with the reflux condenser attached is shown in Figure 6. Reactants were charged through the opening made available by removal of the condenser. The product was withdrawn from the valved bottom opening.

A trial run was made to check operability and ability to anticipate and control the exotherm of the prepolymerizing reaction. This was followed by run No. 5 GR-2 to make prepolymer from HP-370 polyol and p, p'-diphenyl methane diisocyanate at an - NCO/-OH ratio of 0.3. Although the exotherm caused an initial overshoot by about 15°K of the scheduled cook temperature of 398°K, no real difficulty in control was experienced. After the two hour cook, cooling was effected by cutting off steam and slowly adding acetone through the reflux condenser with the stirrer continuing to operate. Acetone refluxed vigorously and most of the cooling from 398°K was effected by the reflux. At the same time the concentration of acetone in the prepolymer was built up as the reactor contents cooled. In the trial run difficulty was experienced with product viscosity rising too rapidly in cooling and stalling the stirring motor. However, in run No. 5 GR-2, smooth "cutting" of viscosity with acetone during cooling was realized. The product was discharged at a temperature 303 - 313°K. The prepolymer recovered amounted to about 20.41 kg as an 80 percent solids in acetone solution.

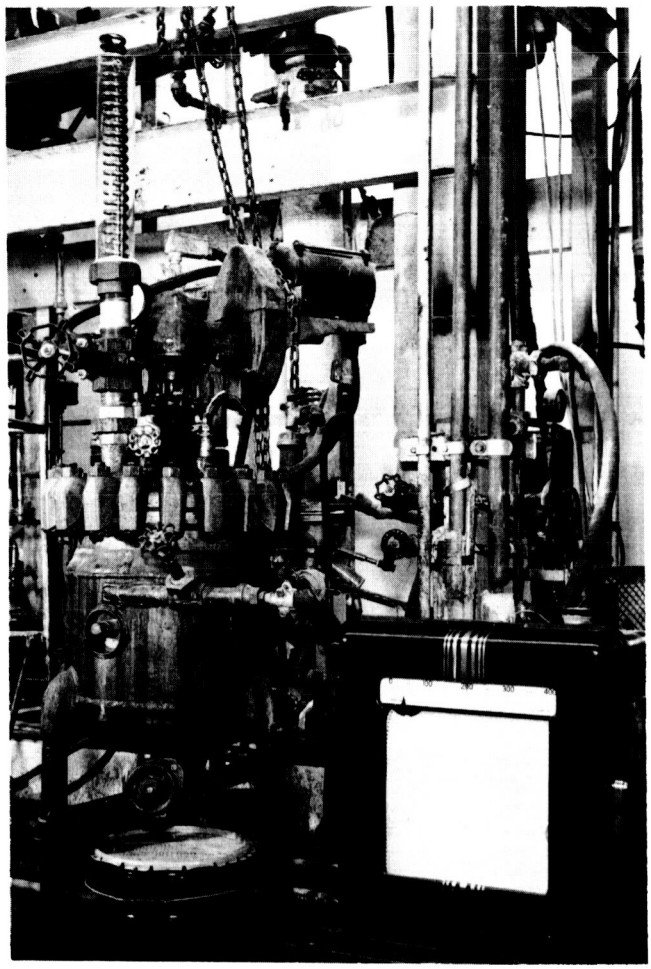

Figure 6. - Steam-jacketed reactor with reflux condenser attached.

Prepolymer inspection: The viscosity-temperature relationship for a pre-polymer sample withdrawn from run No. 5 GR-2 before starting the acetone addition closely followed that found in laboratory preparations of prepolymer. When the prepolymer was incorporated into a standard precoat formulation, the hot-bar sticking temperature of the product foam ran 422-428°K, in satisfactory agreement with previous work. In respect to freedom from cloudiness, caused by a small amount of suspended gel, the material appeared definitely better than any earlier smaller scale laboratory preparations.

The product from run No. 5 GR-2 sufficed for all precoat sheeting studies and for production of sheeted precoat for rigidization of 1.52 meter solar concentrators at the Langley Research Center.

Precoat formulation.

Mixing ingredients: No problems were encountered in scaling up batch size of Formulation No. 394-91 from an earlier maximum of about 0.4 kg (beaker and magnetic stirrer plus manual stirring) to 1.8 kg mixed in a 0.009 m^3 stainless steel bowl with a laboratory bench size dough mixer.

De-acetonizing: Experimentation with 1.8 kg batches established that slurries could be de-acetonized in vacuum satisfactorily if spread in thin layers carrying about 3 kg solids/m^2. Shorter drying times could be obtained with higher vacuum; 81044.4 N/m^2 vacuum for 3 days at room temperature gave a satisfactory product that appeared not to have suffered undue degradation of azide while in contact with acetone.

Sheeting of precoat: The most expeditious approach to producing the required 2.09 m^2 of precoat sheet for each concentrator to be rigidized appeared to be the use of a laboratory hydraulic press. This method was chosen after some preliminary consideration was given to other procedures and a test had been made of sheeting with a 2-roll mill with the rolls at room temperature. Had considerably larger quantities of sheeted precoat been required, a more extended study of sheeting procedures would have been desirable.

Bonding of aluminum backup structure to predistributed foam surface. - Since an added support was required to handle the rigidized solar concentrator in a 1-g environment, it was necessary to devise a means of tying the rigidized mirror to the backup structure without imparting distortions to the mirror. In previous solar concentrator work, this has been successfully accomplished by a foam-in-place bonding of the two structures. Distortions due to the pressure of foam expansion have been minimized by the development of a programmed pattern of localized foaming, using carefully controlled quantities of material. Such a programmed system was developed for this application.

An adequate bond was made using a rigid urethane foam, but to obviate distortions induced by foam shrinkage, a modified flexible foam system was considered and tried. A minimal amount of foam was used to effect the bond in order to limit the increased weight and to reduce shrinkage problems.

The formulation which exhibits acceptable properties is:

50	PBW NIAX Polyol LG-168
50	PBW NIAX Polyol LHT-240
4	PBW Y-4349 Surfactant
2	PBW Y-4499 Cell Opener
2	PBW H_2O
.25	PBW T-9 Stannous Octoate
52.1	PBW Toluene Diisocyanate

Seam Development

General. - At the beginning of this contract, the state-of-the-art of making good quality seams in 2.54×10^{-5} m polyimide film required significant upgrading. Seams had been made which structurally satisfied the requirement but were marginal in integrity, not only from a structural standpoint but also in reflective surface characteristics. Seams previously made had pits and blisters which resulted when exposed to temperatures approaching 450°K during the foaming operation. Thus, the seam development task was included herein for the purpose of improving this general condition.

This task was started by first making a survey of prominent candidate adhesive systems not previously evaluated. The potential systems were assigned individual numbers (H-1, H-2, etc). The constituants of each H-numbered system is described in Table I. The data accumulated through the various tests conducted is documented in terms of the H numbers.

The candidate adhesive systems were evaluated through a series of tests which measured tensile lap shear, peel, creep, and blistering properties of representative specimens. These tests were conducted at room temperature

Table I. - Description of H-numbered adhesives.

Code	Type Sample	Adhesive Coat
H-1	40 PBW #46971 duPont Adhesive 1 PBW #RC805 duPont Catalyst 36 PBW Trichloroethylene 5 PBW Dimethylformamide	1 Spray Coat
H-2	Same as H-1	2 Spray Coats
H-3	40 PBW #46971 duPont Adhesive 1 PBW #RC805 duPont Catalyst $2\frac{1}{2}$ PBW Trichloroethylene	2 Brush Coats
H-4	CMC-11*	1 Ply Unsupported Tape
H-5	Mystik #7361	1 Ply Unsupported Tape
H-6	CMC-141S	1 Ply Unsupported Tape

* Curcuit Materials Company

and also at 478°K, which provided an ample margin in consideration of the 436°K temperature ultimately realized in the vacuum foaming operation.

The following paragraphs describe these tests, and the results obtained. All tests were conducted on specimens made from aluminized Kapton film since it was known that some adhesives behave differently on the bare side of aluminized film than on the same type film that has not been through the vacuum metallizing process. One of several differences in physical characteristics of the two materials is a difference in their retention of a static charge. Also, the conditions the materials experience during the vacuum coating process may contribute to the difference in behavior of the aluminized polyimide film and the non-aluminized polyimide film.

Tensile lap shear tests. - The tensile lap shear samples were 2.54 cm. wide with a 2.54 cm. lap joint and a gage length of 15.24 cm. The load rate was 6.2 cm. per minute and the specimens were soaked at test temperature (room temperature and 478°K) for 3 minutes prior to testing. The adhesives tested were H-4 and H-6 (heat sealed at 505°K) and H-1 and H-5 (pressure sensitive). These test results are given in Table II.

Peel tests. - The peel test samples were 5.08 cm. wide with a 5.08 cm. lap joint. The jaw separation rate was 5.08 cm. per minute and the samples were soaked at test temperature (room temperature and 478°K) for five minutes. The adhesives tested were H-1, H-2, H-3, and H-5. The test results are given in Table III.

Creep tests. - Specimens for the creep tests were prepared like those for the tensile tests. A constant load of .48 kg per cm. was applied. This is the actual load that the material was subjected to during the rigidizing process. At room temperature .48 kg per cm. represents 11 percent of the film strength while at 478°K., .48 kg per cm. represents 16 percent of the film strength and approximately 30 percent of the seam strength.

Figure 7 shows typical elastic deformations and 5-minute creep curves for controls and seams at room temperature and at 478°K. At room temperature no significant creep may be expected after 3 or 4 minutes at the .48 kg per cm. load. However, at 478°K, creep continues after 5 minutes.

In Figure 8 it is noted that the controls approached zero creep rate within one hour (at 478°K) while the seam specimens continued to creep at a very definite rate. One hour tests were adequate to provide creep information for this application since, in the actual rigidizing process, the seam would be exposed to the high temperature for approximately one minute before the cool-down was to start. The curve shows that for a 5-minute period at 478°K the creep would be 0.5 mm, which in this application is negligible.

Table II. - Tensile lap shear test results.

Type Sample	Ultimate Load (kg)			Adhesive Coat	Test Temp
	Min	Max	Avg[b]		
Polyimide Film[a]	11.4	12.5	11.8	None	RT[c]
Polyimide Film[a]	6.1	7.3	6.5	None	478°K
H-5	8.9	11.2	9.9	1 ply	RT
H-5	3.3	3.8	3.6	1 ply	478°K[d]
H-4	10.9	12.6	12.0	1 ply - heat sealed	RT
H-4	2.9	3.6	3.3	1 ply - heat sealed	478°K
H-6	10.9	11.9	11.5	1 ply - heat sealed	RT
H-6	4.4	5.3	4.8	1 ply - heat sealed	478°K
H-1	12.0	13.7	12.8	1 spray coat - heat sealed	RT
H-1	3.9	4.4	4.1	1 spray coat - heat sealed	478°K
H-2	8.8	12.9	10.4	2 spray coats - heat sealed at 505°K	RT
H-2	3.4	4.2	3.9	2 spray coats - heat sealed at 505°K	478°K
H-3	11.7	12.5	12.0	1 spray coat 1 brush coat - heat sealed	RT
H-3	3.4	4.1	3.8	1 spray coat 1 brush coat - heat sealed	478°K

Notes:
a Control sample.
b Average ultimate load is for five samples.
c RT - room temperature.
d During 478°K testing all failures occurred

Table III. - Peel test results.

Type Sample	Ultimate Load (kg)			Adhesive Coat	Test Temp
	Min	Max	Avg		
H-5	.45	.52	.50	1 ply	RT
H-5	.07	.08	.07	1 ply	478°K
H-2	2.27	6.4	4.1	2 spray coats - heat sealed	RT
H-2	.09	.48	.28	2 spray coats - heat sealed	478°K
H-2	.68	1.1	1.0	2 spray coats - contact bonded	RT
H-2	.06	.13	.11	2 spray coats - contact bonded	478°K
H-4			.11	1 ply	RT
H-4			.06	1 ply	478°K
H-6			.14	1 ply	RT
H-6			.06	1 ply	478°K

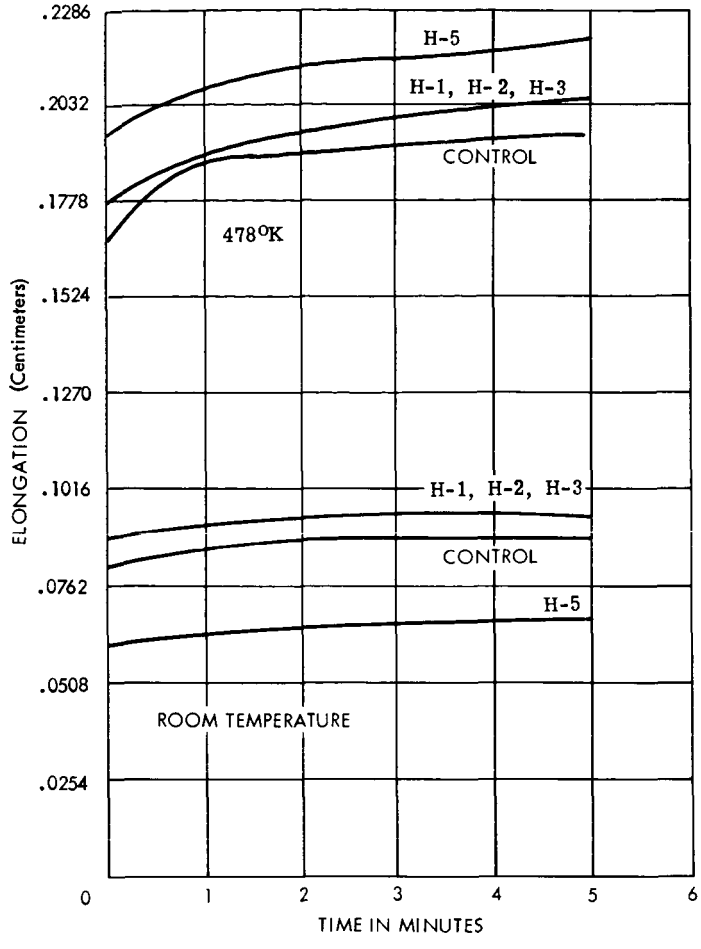

Figure 7. - Creep tests of H film adhesives.

Blistering test. - Blistering test samples were made with 25.4 cm diameter discs with a seam across the diameter. Precoat foam material was applied to the samples. They were then clamped in a pressurizing fixture which was installed in a vacuum chamber. The chamber was evacuated and the samples pressurized which applied a load to the seam. The precoat material was activated and the samples were rigidized in a dome shape. Three different pressures were used in three different tests in which the load was varied from .48 to .72 to .89 kg per cm. In each case, only negligible evidence of pitting, blistering, or separation was noted.

A review of the physical test data on the various seaming materials shows that the H-2 adhesive, applied in two coats by spraying and heat sealed at 505°K, was superior to the other adhesive systems. Its tensile lap shear test results ranked second only to the H-1 results while the

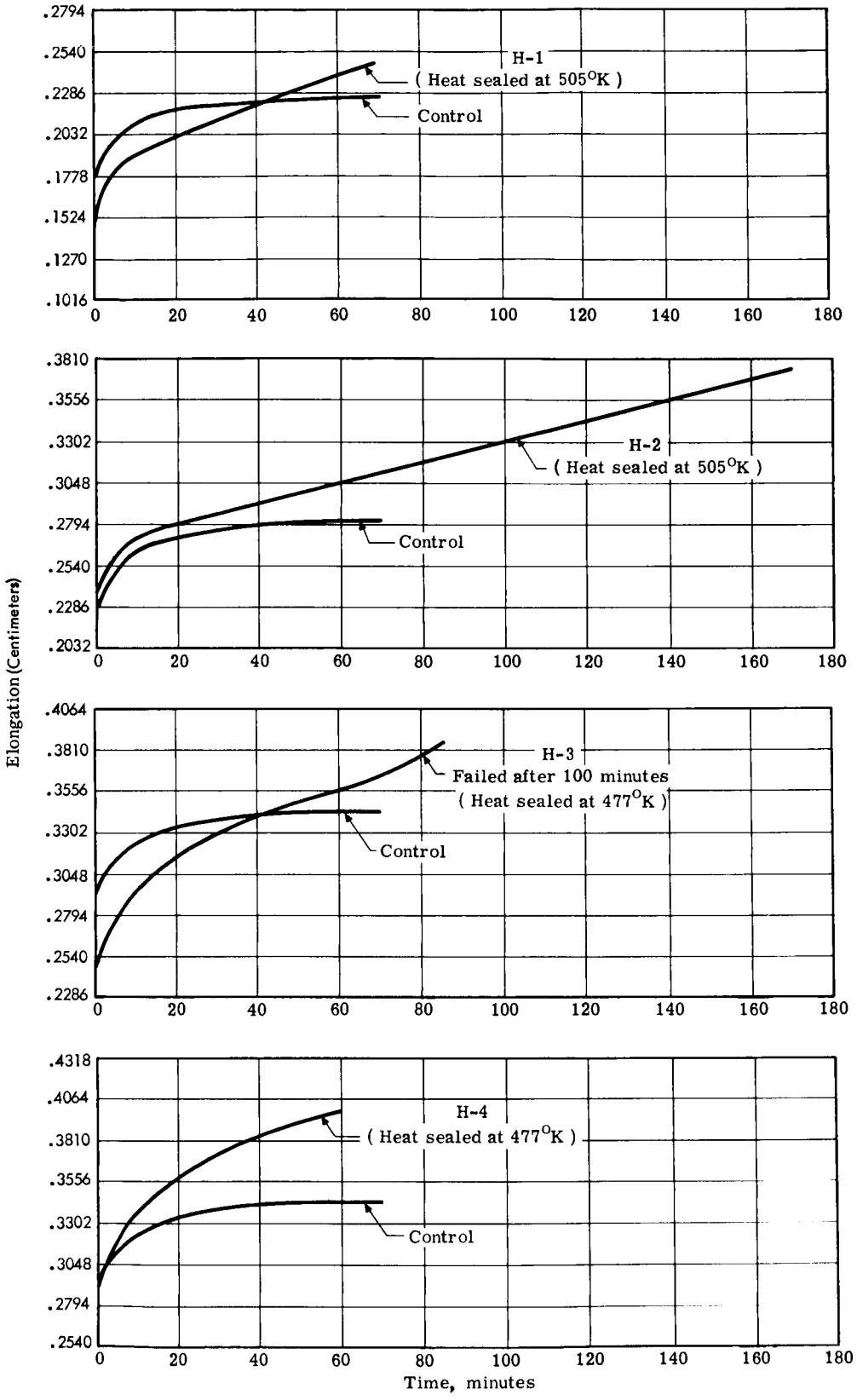

Figure 8 (Sheet 1). - Creep tests on H film adhesives at 478°K.

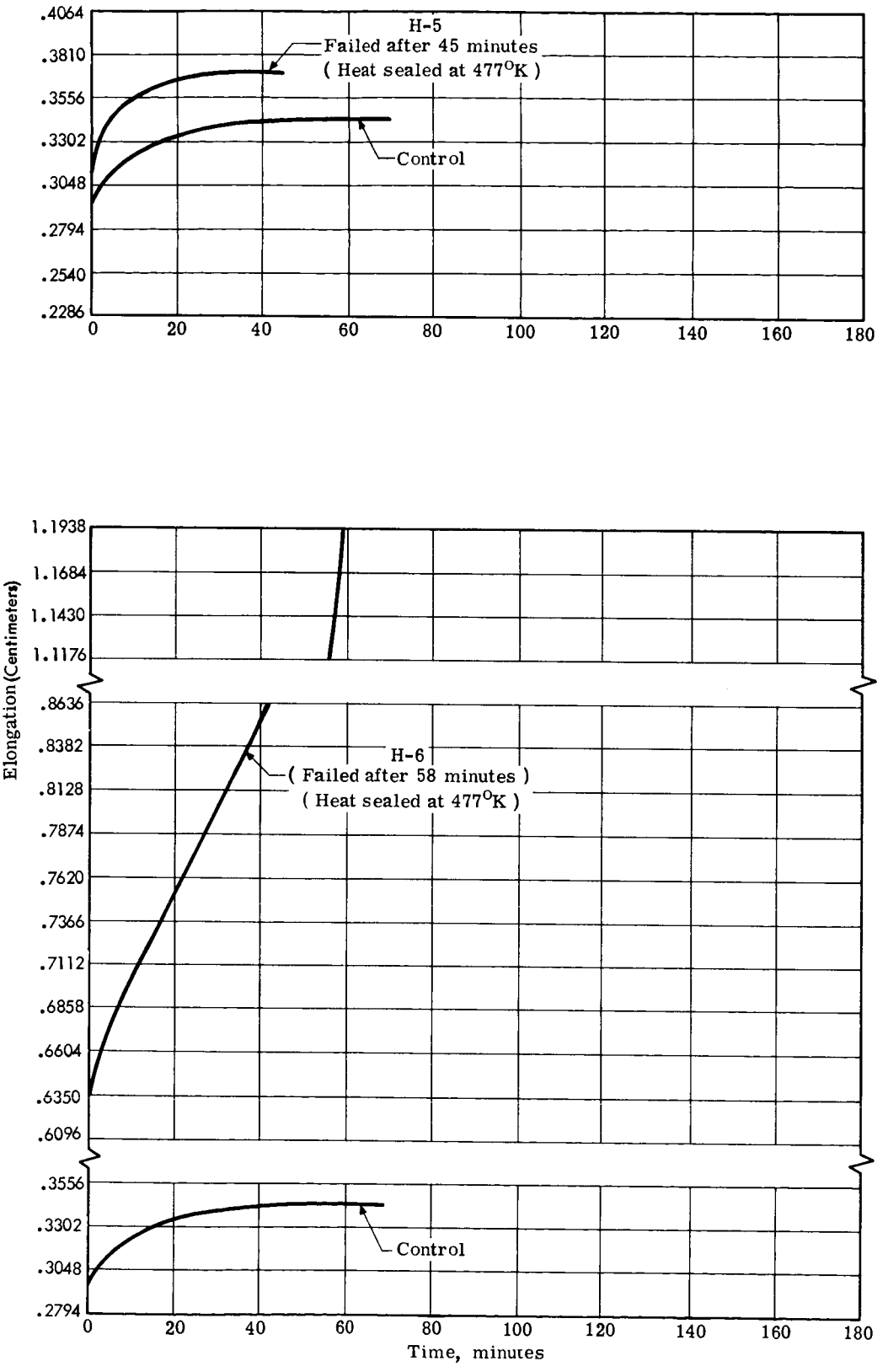

Figure 8 (Sheet 2). - Creep tests on H film adhesives at 478°K.

peel tests ranked first. The creep test results shows the H-2 adhesive to have a clear advantage lasting over 160 minutes before failure while, the next best, H-3 system failed after 100 minutes.

Based on these results, the H-2 adhesive and sealing system was selected for use for the mirror fabrication.

Fabrication

General. - Two solar concentrators were constructed for this program. This construction necessitated the development of detail manufacturing procedures, and also the design and fabrication of a test fixture for restraining the test article and performing related tasks. Several sub-assemblies were fabricated prior to the installation of the test articles into the fixture for completion in the vacuum chamber. The procedure was as follows:

(1) Design and build test fixture.

(2) Make precoat sheet material in segments to ultimately cover inflated film in mirror area.

(3) Make polyimide film sub-assembly.

(4) Make ring type backup structure.

(5) Ship above items to Langley Research Center for use in 18.29 m diameter vacuum sphere.

(6) Install test fixture in chamber.

(7) Install film sub-assembly on fixture and inflate.

(8) Apply pre-coat sheet to back of film.

(9) Complete setup by checking contour, making necessary adjustments, and putting heat source in place.

(10) Evacuate chamber and apply heat, causing foaming of precoat material.

(11) Bring chamber to ambient pressure.

(12) Add backup structure using low modulus urethane foam system.

(13) Remove mirror from fixture.

The above steps are individually described in subsequent paragraphs.

Test fixture design and fabrication. - This test fixture was provided for the rigidization of the 1.52-meter diameter parabolic concentrators in the vacuum sphere. The test fixture had to serve numerous functions as described below.

(1) Provide accurate location and support of the inflatable membrane throughout the test cycle. The membrane attachment to the test fixture simulated attachment to an inflated sphere or lenticular shape.

(2) Provide a means for precise adjustment of the contour prior to the rigidization task.

(3) Provide means for accurate pressure control without leakage through the structure before, during, and after exposure to the vacuum environment.

(4) Provide a means for accurately measuring the contour of the parabolic shape at specific predetermined radii at any time that the membrane was attached to the fixture. Also, provisions had to be made to permit retraction of this measuring device while attaching the membrane or removal of the mirror to prevent damage to the mirror surface.

(5) Provide means for exposing the foamable composition to a controlled heat flux to initiate and control the foaming action.

(6) Provide means of measuring the temperature of the foam composition at pre-determined points in the foamable material throughout the foaming process.

(7) Provide means for visual inspection of the mirror surface while attached to the test fixture.

(8) Provide access for attachment of a backup structure to the completed reflector prior to removal from the test fixture.

(9) Provide means for controlling these systems from outside of the vacuum sphere.

The test fixture, designed and fabricated to satisfy these functions, is shown in Figure 9. In this photo the major components are in place with the exception of the heater and the membrane clamp ring. The heating element is shown in Figure 10.

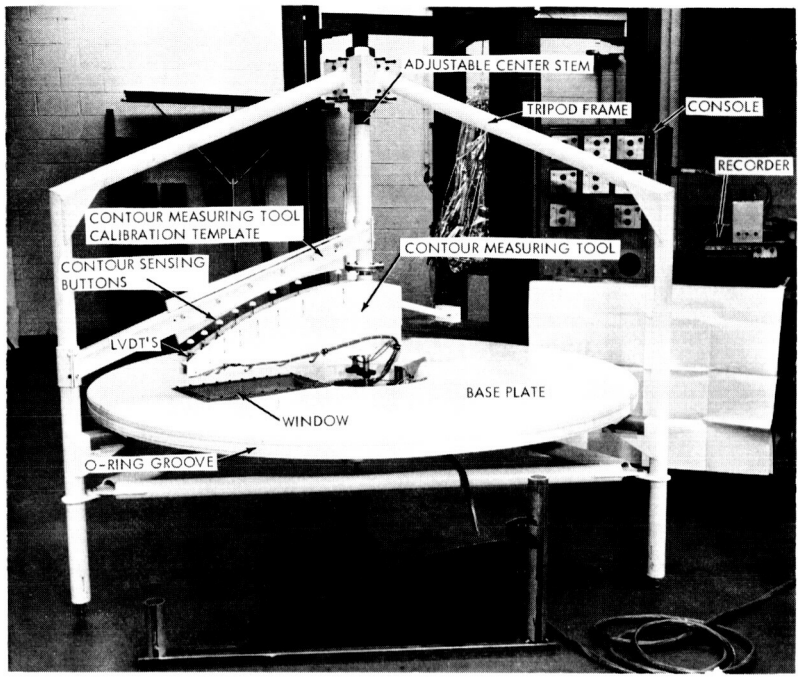

Figure 9. - Membrane mounting and alignment system.

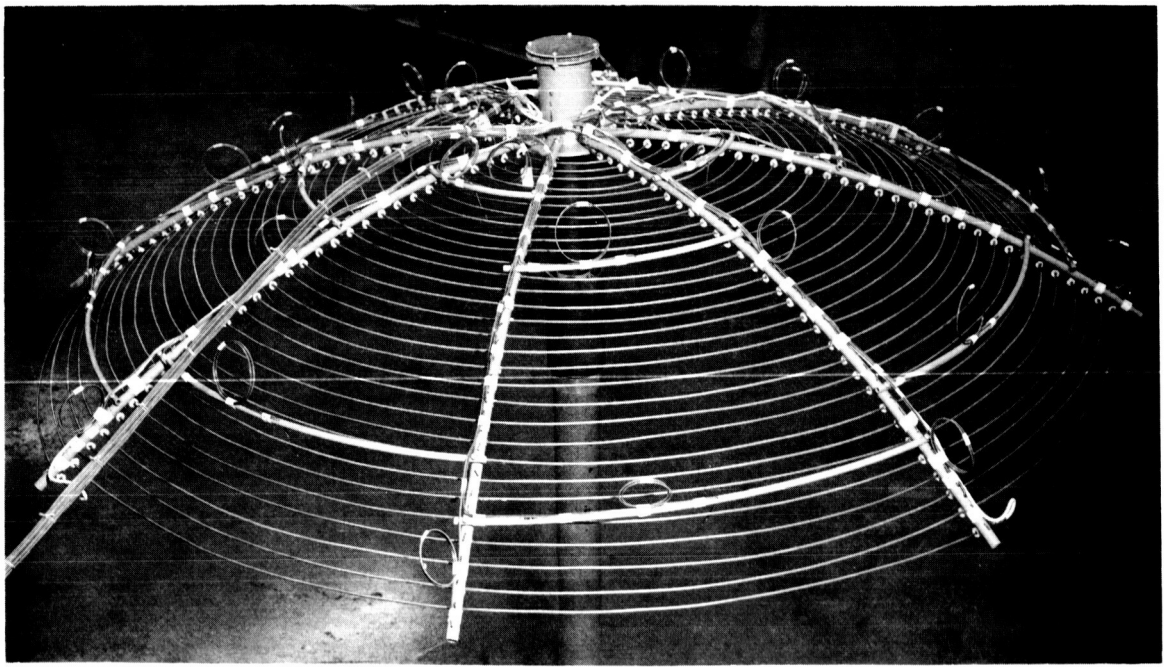

Figure 10. - Heating element and thermocouple arrangement.

This test fixture consists of a tripod type frame assembly to which is attached a 2.134 meter diameter base plate. The base plate serves as a closure to which the inflatable membrane is attached, and has an O-ring type groove around the periphery for sealing the membrane. A two piece clamp band with a matching groove clamps the membrane to the base plate. This base plate also contains a plexiglass window for visual observations. In the center of the base plate is the mechanism for raising and lowering the contour measuring arm, through a distance of 5 cm. This center plate also contains a 5 cm diameter air line port for the pressurization system, and the port for differential pressure transducers. A recess is provided in the center area of this plate for the contour measuring arm drive unit. Attached to the three vertical leg members of the tripod are three additional structural members which support a hub fitting at the center, above the test article. This hub is for the purpose of locating an adjustable center stem for attachment of the membrane hub, the heating element, and the contour measuring tool (see Figure 9).

The adjustable stem of this fixture has a minimum travel of 0.9 cm in the horizontal plane and a minimum travel of ± .25 cm in the vertical plane.

The heating element mounts on the stem, and is adjustable through 60 cm in the vertical direction. This movement provides a means for stowing the element in a position far enough above the membrane to permit convenient installation of the membrane and subsequently the foamable material. The heater can then be lowered to its desired position during the foaming phase. This heating element consists of a spiral winding of two parallel circuits of 9 gauge (0.29 cm diameter) heating element wire having a resistance of 0.2208 ohms per meter. The heating element has an outside diameter of 1.57 cm. A spacing of 2.54 cm was maintained between wires. Each circuit contains 46.1 meters of wire. The support arms for the heating element describe the same contour as the theoretical parabola being used. The heating element is attached to the support arms by porcelain coated hooks. All soldering was done with silver solder, and mechanical junctions were provided where possible. This heating element also provides the support for 36 copper-constantan thermocouples which were utilized to monitor the temperature of the foamable material throughout the foaming cycle. These thermocouples were attached by means of a high temperature glass fiber tape and were so located that each monitored an equal surface area.

The contour measuring tool is comprised of an arm which extends from, and rotates through 360° on the stem attached to the frame assembly. This arm carries eight vertically mounted Linear Variable Differential Transformers (LVDT's). On the lightly spring loaded movable plunger of each is mounted a spherical button which contacts the inflated mirror.

The inductance of the LVDT is determined by the vertical position of the plunger, which is in turn dependent upon the button position as it contacts the mirror. Thus the LVDT's measure the difference between the actual and theoretical parabola. Figure 9 shows the contour measuring arm during calibration. A template defining theoretical mirror contour is used to establish zero setting of each LVDT. The LVDT's are located at equal area intervals of the mirror contour.

The support arm can be lowered 5 cm so that the LVDT's will not exert pressure on the reflector membrane during installation of the membrane. Needle bearings are used at the central shaft attachment to insure alignment and yet permit up and down movement. When the arm is in the up position, a spring loaded plate recessed in the arm rides on top of a ball thrust bearing for support of the arm. The arm is driven through a gear mechanism attached to the central shaft and the drive motor. The drive motor is a synchronous type having a speed of 40.2 rps and a torque value of 144,000 gr. cm. The mating torque motor is located in the control console. The mechanism for raising and lowering the arm is located in the center base plate of the frame assembly. All rods used in the raising and lowering mechanism function through seal glands.

The sketch below schematically shows the pressure control system utilized to precisely control the differential pressure within the membrane prior to, during, and after evacuation of the chamber. Through the use of this system, and the ability to monitor the contour using the contour measuring device described above, the membrane shape was accurately maintained throughout the critical period of rigidization.

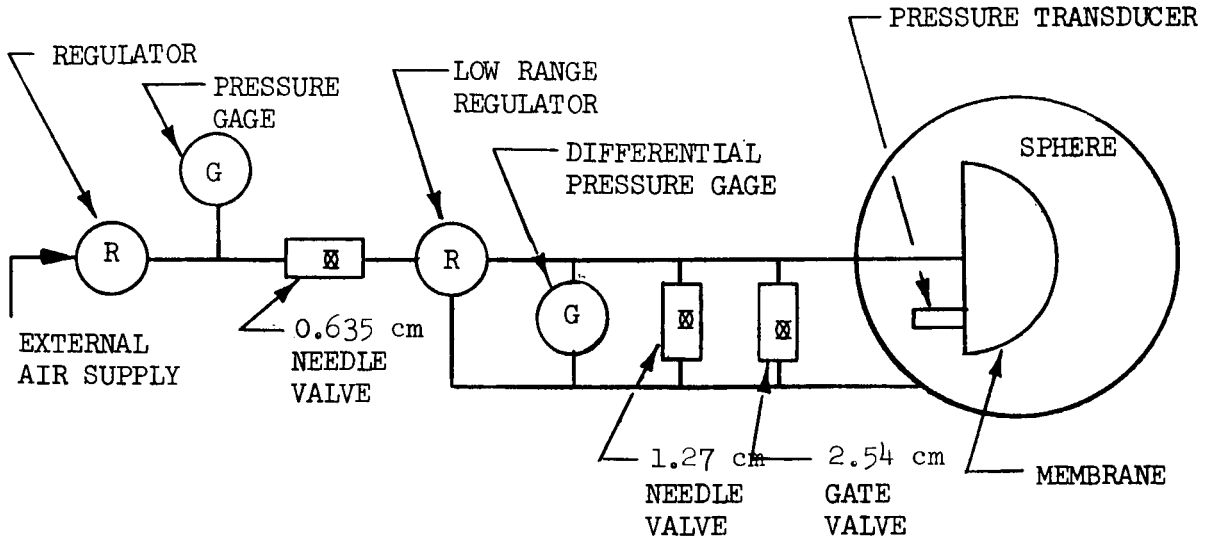

This test fixture was controlled and monitored remotely during use in the vacuum chamber with the console and recording device pictured in Figure 9. This fixture performed satisfactorily on this program.

Material preparation and subassembly.

Membrane fabrication: Three complete membrane assemblies were fabricated at GAC for use on this program. The following paragraph outlines the fabrication procedure used.

The individual gores (24 per unit) of 2.54×10^{-5} m aluminized polyimide film were rough trimmed. The layup operation was accomplished on a 24 segment three-dimensional tool which was available at GAC. The joint between adjacent gores was accurately made by overlapping the adjacent gores and cutting them as one. The scrap was removed and the butt joint sealed with the tape using an iron electrically heated to 505°K. The tape used was 1.27 cm wide with the H-2 adhesive described in an earlier section. Figure 11 shows a unit in process.

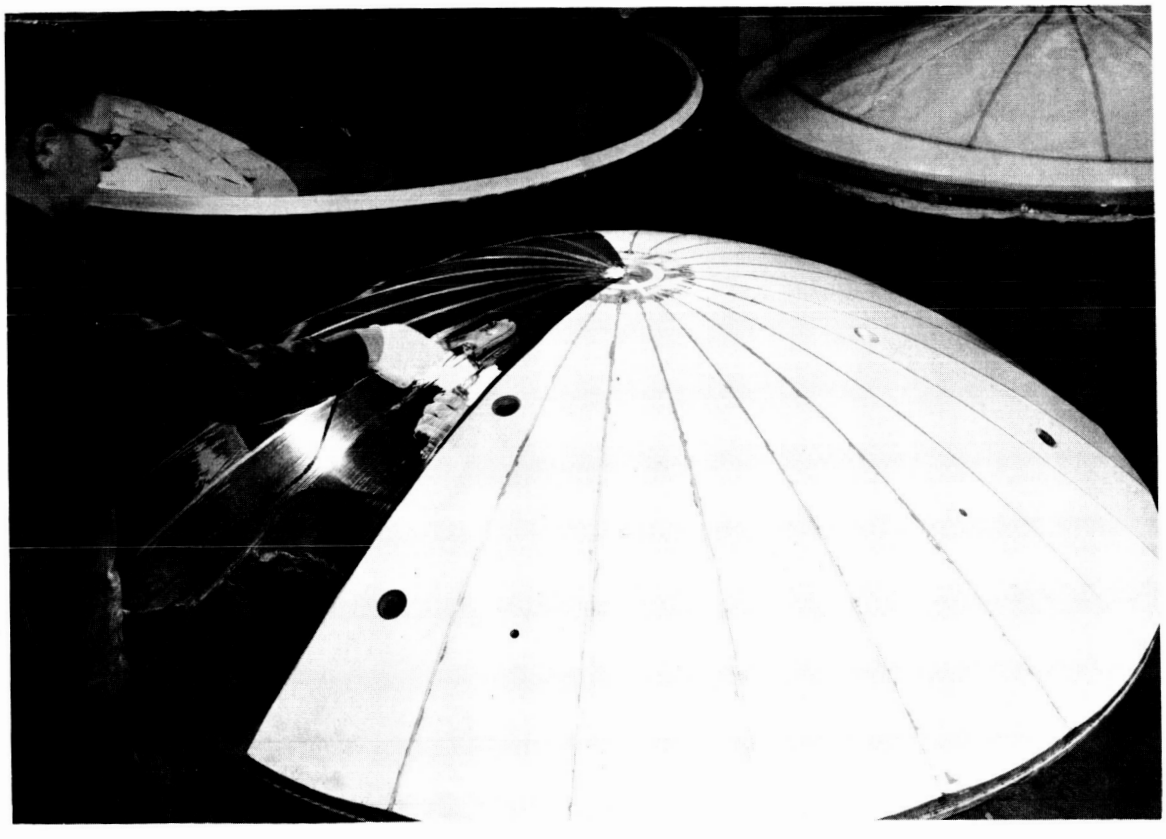

Figure 11. - Partially completed lay-up of gores on mold.

After seaming was completed, the metal hub was attached and securely sealed. The unit was then inflated and inspected. After inflation, it was removed from the mold and mounted on the packing fixture for storage and future shipment.

Preparation of precoat sheet stock: Three like batches of precoat material were prepared for use in rigidizing 1.52 m reflectors. These batches were carried individually through the mixing, de-acetonizing, and sheeting operations. The batches were numbered 1, 2, and 3 in order of preparation. In the work at LRC, the preliminary unit was rigidized with batch No. 3 and the final unit was rigidized with batch No. 2. The spare batch of material (No. 1) was not used.

The precoat batches were formulated to reproduce the chemical composition represented by Formulation No. 394-91 that had been developed in earlier work. This formulation is shown in table IV.

Some scaling-up and changes in techniques were involved in preparation of the three batches of sheeted precoat in comparison with earlier work. This was a consequence of the approximate six-fold increase in concentrator area to be rigidized.

Table IV. - Precoat formulation No. 394-91

Component	Parts by Weight
Hydroxyl-terminated prepolymer	55.4
Azide structure X	16.5
Bisphenol adduct of 4.4' - diphenyl methane diisocyanate[a]	26.0
Surfactant L-5310[b]	1.6
Tin catalyst D-22[b]	0.5
	100.0
Quartz fiber (0-3 micron diameter)[c]	2.0
Acetone (for plasticizing during mixing)	33 to 40

[a]Supplied by E. I. du Pont
[b]Supplied by Union Carbide
[c]Supplied by Johns-Manville

Prepolymer prepared in run No. 5GR-2 was used. Each of the three batches was formulated to contain 1.82 kg solids. Mixing was done in a nominal 9.463 0.009 m^3 kettle with a mixer using medium speed for 30 - 40 minutes. Immediately after mixing, each batch was spread over an area of about 0.61 m^2 in aluminum foil-lines trays. The trays were then placed in a chamber at room temperature and held at about 81326.7 N/m^2 vacuum until de-acetonized to the point that the material was non-tacky to the touch. This required about three days under vacuum. It is known from previous work that a non-tacky state of the precoat at room temperature implies an acetone content under one percent. Hence for practical purposes, the observed weights of de-acetonized precoat may be used without consideration of residual acetone.

After de-acetonizing, the material somewhat resembled a rough and porous taffy sheet with an average weight per unit area of 3 kg/m^2. This sheet was then cut into sections and pressed into sheets of approximately 0.51 mm thickness with a target weight per unit area of about 0.65 kg/m^2. A 50-ton hydraulic press with 30 x 38 cm. electrically heated platens was used in this operation. It was found that the material could not readily be pressed to the desired thin, uniform sheet with platens at room temperature; so it was necessary to press with platens heated to 311 - 316°K and a pressure of around 100 kg/cm^2. Still higher platen temperatures would have further eased the time-pressure conditions for pressing, but lacking full information on azide stability, it seemed best to work at the lowest possible temperature. Pressing was done with 2.54 x 10^{-5} m polyethylene film sheets on either side of the precoat. The sheets facilitated handling while trimming to specified block sizes after pressing, and then served as separators during storage and transportation of the finished blocks. The sheets were finally removed (peeled off) at the time of applying the blocks to the membrane of a concentrator.

The time periods involved in preparing and storing the various batches of sheeted precoat are given here.

	Batch No.		
	1	2	3
Processing time (mixing to completion of pressing and trimming), days	11	18	8
Storage time for batch, days		16	7
Age of batch when foamed, days		34	15

After mixing and de-acetonizing, all material was held at about 280°K for as long as possible.

Back-up structure design and fabrication: The single analysis summarized below was performed to determine the structural requirements of the back-up structure in a 5.14 m/s wind condition.

$$N_\phi = \frac{Fq}{\cos \phi}$$

$$N_\theta = \frac{2\,Fq}{\cos \phi}\left(1 - \tfrac{1}{2}\cos^2\phi\right)$$

where F is the focal distance and the other quantities are shown in Figure 12. The focal distance is given by:

$$F = \frac{r}{2}\cot \phi$$

$$\therefore\ F = \frac{1.52}{4}\cot 30^\circ = .38\sqrt{3} = .658 \text{ m.}$$

For a 5.14 m/s wind load $q = 1.66$ kg/m^2

$\therefore$ The maximum membrane forces, (which occur at the edge) are:

$$N = \frac{.658 \times 1.66}{\cos 30^\circ} = 1.26 \text{ kg/m}$$

$$N_\theta = \frac{2 \times .658 \times 1.66}{\cos 30^\circ}\left(1 - \tfrac{1}{2}\cos^2 30^\circ\right) = 1.57 \text{ kg/m}$$

On the basis of these low stress levels, a simple ring structure was designed and built. The ring was 2.54 cm diameter aluminum tubing, and contained three equally spaced pads for attachment of the mirror to the supporting structure. The ring was designed such that it could be brought to the mirror in two pieces and spliced together after being placed in position against the foamed back of the mirror. Thus, the mirror could be supported by the inflation pressure until the back-up is completely attached. The planned attachment was by use of a low modulus rigid foam which would adhere to the mirror foam and simply encapsulate this ring except at the three attach points.

Setup/pre-vacuum operations: The test fixture assembly (Figure 9) was built and checked out at GAC and then shipped to NASA Langley for utilization in the 18.29 m diameter vacuum chamber. The program plans called for a preliminary and a final 1.52-meter diameter concentrator to be rigidized in a vacuum environment. The setup/pre-vacuum operations were the same for both mirrors and consisted of (1) membrane installation, (2) membrane pressurization, (3) membrane alignment, and (4) application of pre-coat and instrumentation.

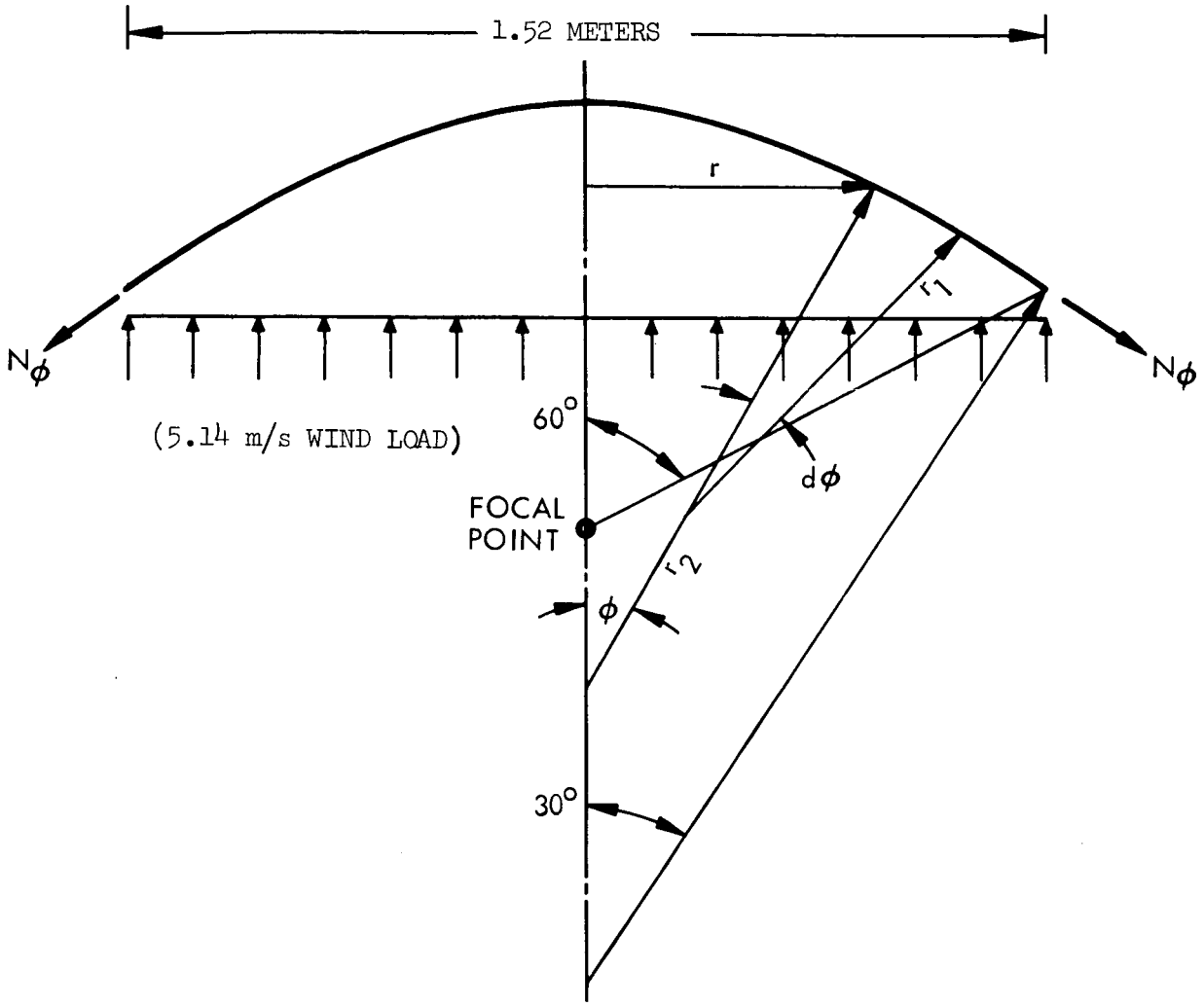

N_ϕ = NORMAL STRESS KG/M IN RADIAL DIRECTION
N_θ = NORMAL STRESS KG/M IN CIRCUMFERENTIAL DIRECTION

Figure 12. - Side view of paraboloid showing stresses in radial direction.

Membrane installation: The contour measuring arm and the dummy hub were removed from the test fixture assembly. The seal gasket was placed on the hub and the hub was mounted to the stem of the frame assembly with gore seam No. 1 pointed at frame assembly leg No. 1. During fabrication, a specific gore with respect to the mold and the hub was marked as gore No. 1. This provided a mold-hub orientation for all mirror membranes. This mounting of all mirror membranes in an identical position eliminated the amount of readjustment required. The contour measuring arm was then bolted to the hub and stem assembly, caution being taken to keep the rotating portion of the arm in the down position. Care was taken at all

times to eliminate any wrinkling of the membrane. Gloves were worn at all times and shirt sleeves rolled down to eliminate fingerprints or smudges on the mirror surface.

The membrane was stretched over the edge of the base plate with surgical tubing utilized as an O-ring in the plate O-ring groove. The gore extending over the contour measuring arm was placed first and the remainder of the mirror worked in both directions from gore No. 1. With the O-ring in place the membrane was inflated to a pressure of approximately 124.4 N/m^2 This inflation was sufficient to pull the O-ring tight against the upper part of the O-ring groove. Then the two-piece clamp band was installed. Both joints of the clamp band were tightened equally and intermitently at opposite sides to keep an equal pressure on the O-ring and to eliminate wrinkling of the membrane. Small rubber pads were installed in the clamp band joints to prevent any leakage in these areas.

Membrane pressurization: To pressure the membrane at ambient conditions, external air was used. This was accomplished by attaching a shop air line to the pressure regulation system. The high pressure regulator was adjusted to allow a pressure of 1 atmosphere on the low pressure regulator shut-off valve. Both bypass valves were closed. The shut-off valve to the low pressure regulator was then opened. The low pressure regulator was allowed to operate full open until the membrane was full. Then the regulator was adjusted to maintain 124.4 N/m^2 pressure until the clamp band was installed.

Once the clamp band was installed, the low pressure regulator was adjusted to give a differential pressure of 51 mm of water. At a differential pressure of 497.7 N/m^2 the shut-off valve to the low pressure regulator was closed and a leak check was made. Where membrane leaks were suspected, a soapy water solution was used to check for leaks. All leaks were repaired.

The low pressure regulator was then adjusted to maintain a differential of 273.7 N/m^2. Earlier tests had indicated this was the optimum membrane pressure for foam rigidization.

Membrane alignment: With a differential pressure of 273.7 N/m^2 established, a contour measurement of the membrane was made. This first measurement of the contour was primarily for determining concentricity of the parabola. When the best concentricity of the membrane was obtained, additional measurements were made to determine if the membrane had the proper parabolic shape. Adjustments to change this feature of the membrane were made by raising or lowering the stem in a vertical direction and by increasing or decreasing the differential pressure in the membrane. From prior knowledge of the membrane movement during the foaming process, it was known that the foaming operation would tend to cause slight contour change creating a slightly longer focal length effect. Therefore, the initial setting should be aimed at a shorter focal length to compensate.

The differential pressure of 273.7 N/m^2 was maintained during the application of the precoat material. Figure 13 shows the membrane inflated and ready for precoat.

Application of precoat and instrumentation: With the membrane established at its optimum contour, the outer surface of the membrane was washed down with a solution of methylethyl ketone (MEK) and allowed to dry.

Sheeted precoat material was unpackaged and applied to the membrane area to be rigidized. This area, amounting to 2.09 m^2, was bounded by the hub (0.15 m diameter) and by a circle of 1.57 m diameter. To cover this area, 67 precut flat blocks of precoat sheet were applied in four tiers as follows:

hub tier - 8 blocks

second tier - 14 blocks

third tier - 20 blocks

rim tier - 25 blocks

All blocks in a tier were identical in size (trimmed on the same pattern), but size and configuration varied somewhat from tier to tier. The configuration may be described as a flat, four-sided figure with two opposing sides approximating meridians on a sphere and the other two sides parallels on a sphere.

The inherent discrepancies between a surface with three-dimensional curvature and blocks cut to flat patterns gave very little trouble. In some cases, however, to close a tier it was necessary to trim the side of the last block or to add a narrow filler strip.

All blocks were kept cool until they were unwrapped immediately before use, to prevent them from becoming tacky.

The plasticity of the blocks permitted them to conform quickly to the contour of the inflated mirror membrane after being set in place, and the surface of the blocks possessed sufficient tackiness that, once set, they would remain in place. Thickness of the precoat blocks was about 0.51 mm ± 5 percent; weight/unit area was 0.62 kg/m^2 ± 5 percent. Figure 14 shows the precoat in place.

Following application of precoat material, the heating element was lowered into position. With the membrane not assuming a true parabolic shape, the heating element did not follow its exact contour. On mirror No. 1 the heating element was approximately 2.5 cm from the precoat material at the edge of the mirror and 5 cm from the precoat material at the hub. During the foaming process, one of the safety wire attachments

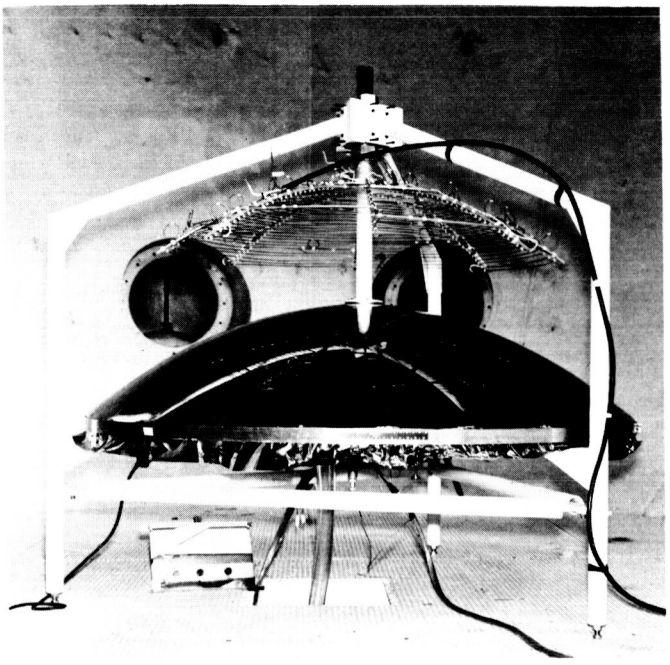

Figure 13. - Inflated membrane.

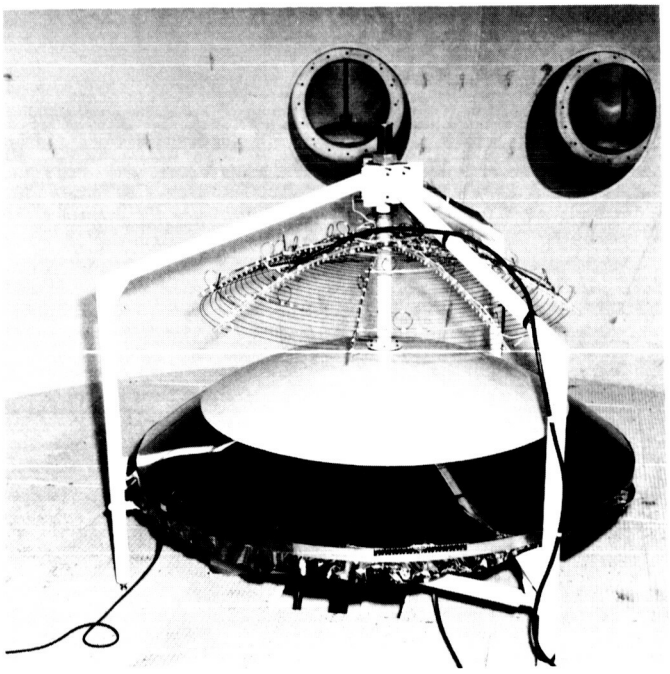

Figure 14. - Inflated membrane with precoat installed.

on the heating element frame slipped and one portion of the outer edge dropped to about 1.3 cm from the precoat material. During exotherm, the membrane expanded and the foam material actually encapsulated part of the heating element. On mirror No. 2 the portion around the hub was placed at 5 cm from the material. Turnbuckles were placed on all heating element arms to draw them up so the outer edge was also 5 cm from the precoat material.

There were 36 thermocouples attached to the heating element structure. These thermocouples had silver solder junctions. On the preliminary unit these thermocouples were positioned so that they were pointing almost perpendicular to the membrane. When the membrane expanded during the foaming process, all thermocouples formed a very distinct raised mound on the mirrored surface of the membrane. In fact, one of the thermocouples actually punctured the membrane. On the final mirror these thermocouples were made with a lead wire approximately 15 cm long from the heating element frame, and stretched out along the surface of the membrane like a long lever arm. When the membrane expanded they actually followed the motion of the membrane. Also, on the final unit, several thermocouples were covered with small patches of precoat material. These thermocouples are all indicated on the thermocouple plot location (see Figure 15).

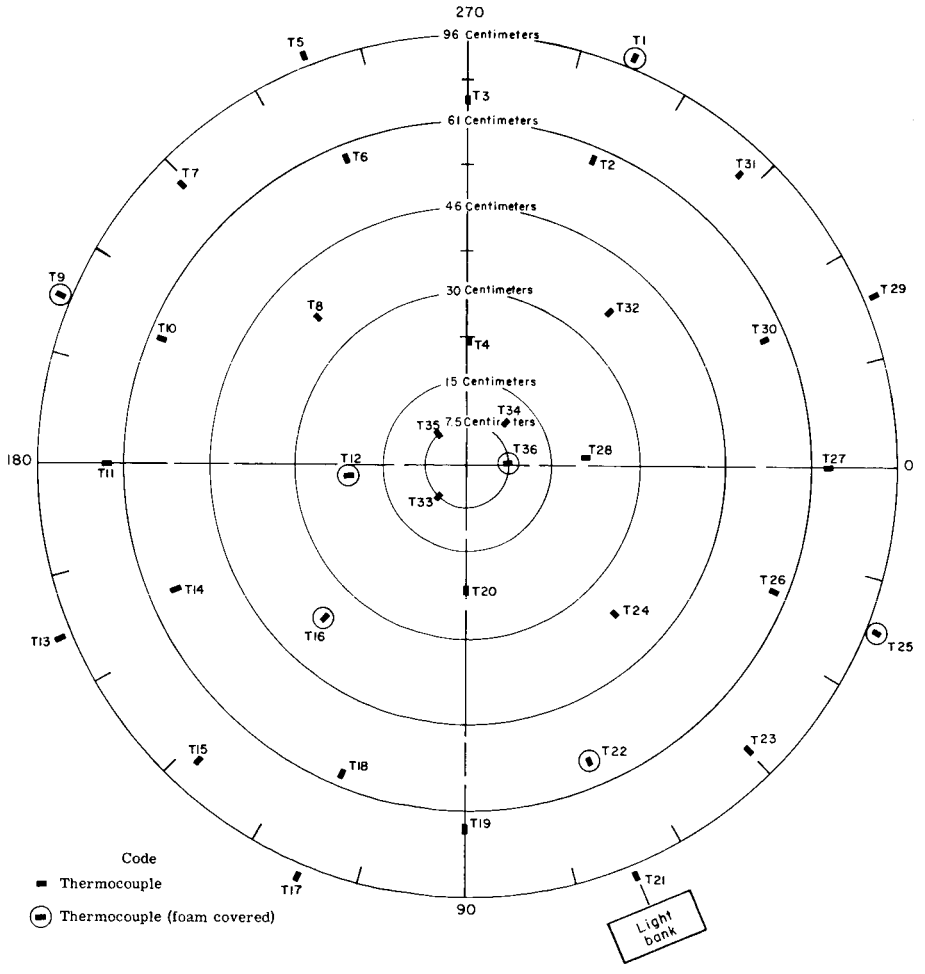

Figure 15. - Thermocouple locations.

Rigidization. - The culmination of this program was the application of the material and process knowledge gained from earlier tasks to the rigidization of two 1.52-meter diameter parabolic mirrors under vacuum conditions. The first of these units was for the purpose of refining the procedures and techniques. The second was the refined product, representing essentially the level of development of the state-of-the-art at this time.

As has been stated earlier, the foam rigidization of the concentrators was carried out in NASA Langley's 18.29 m diameter vacuum sphere. The detailed actions taken to foam rigidize the two concentrators are set forth in the following paragraphs.

Vacuum chamber pump down: The pump-down procedure of the 18.29 m vacuum sphere was similar for both the preliminary and final test articles. When the vacuum sphere was sealed, the external air pressure line connected to the pressure regulation system was disconnected. The high pressure regulator was closed, and the low pressure regulator shut-off valve was closed. For the preliminary unit, the first pump of the sphere pumping system was started. The 2.5 cm bypass valve was opened to bleed air from the mirror membrane into the sphere. With only one pump running, a differential pressure of 248.8 N/m^2 was maintained. Additional pumps were then started one at a time to assure that a 248.8 N/m^2 differential pressure would be maintained in the reflector membrane at all times. It was found that with all six pumps in operation, air could be bled from the mirror membrane fast enough to maintain this differential pressure. As a result, on the final unit all six pumps were used immediately at the start of pump-down.

To prevent possible damage to the first unit due to reverse pressure on the membrane, it was decided to run through the complete foaming process without any shutdown time of the pumping system. Therefore, the pumping process was started at 3:00 a.m. and run till completion. The large bypass valve of the pressure regulation system was gradually closed to maintain the 248.8 N/m^2 pressure differential in the membrane.

When the vacuum in the sphere was such that readings could be made on the micron scale, the large bypass valve was closed and the small bypass valve was opened for fine control of the differential pressure in the membrane. At a vacuum of 20 N/m^2, the pumping system became stabilized until leaks were found in the thermocouple seal glands and sealed. The pumping system then continued to pump down the vacuum sphere until a pressure of less than 0.133 N/m^2 was reached. The foaming process was to be initiated at a pressure of less than 0.133 N/m^2. The preliminary mirror was foamed with an initial reading of 0.09 N/m^2 on the ionization gage. A complete pressure-time history of the pump-hours of the vacuum sphere for this unit is given in Table V.

On the final unit it was decided to attempt a shutdown of the pumping system and hold overnight. Pump-down was started in the early afternoon and reached a vacuum of 11.60 N/m^2 at shutdown time (approximately 4:00 p.m.).

At this time a differential pressure of 248.8 N/m^2 was being maintained on the mirror membrane. Knowing that there would be a minimum amount of leakage into the sphere overnight, it was decided to bleed air into the mirror membrane through the low pressure regulator. The low pressure regulator was set for a minimum pressure of 62.2 N/m^2 water differential. This would maintain a positive pressure on the membrane at all times. The following morning, the vacuum sphere pressure had increased to a pressure of 106.66 N/m^2. The mirror membrane differential pressure was registering 59.7 N/m^2. The membrane appeared to be in satisfactory condition from observations from the sphere ports. On the basis of this, the pumping process was resumed and the sphere reached a prefoaming pressure of 0.03 N/m^2 on the ionization gage. A complete pressure-time history of the vacuum sphere pump-down for the preliminary mirror is given in Table VI.

Precoat foaming operation: Figure 16 is a sequence which shows the foaming operation on the preliminary mirror from start to finish. Figure 17 displays the same operation on the final unit.

When the vacuum sphere was pumped down to less than 0.133 N/m^2 differential pressure of the membrane and the sphere was stabilized at 273.7 N/m^2, a contour measurement was taken. Immediately following this, the heat-up process was begun. The goal was to raise the temperature of the precoat material from ambient temperature to precoat foaming temperature at a constant rate of 6.67°K per minute.

On the preliminary unit, the initial temperature of the precoat material was 299°K. At this time, a voltage of 50 volts ac at 9.5 amperes was applied to the heating element. This was gradually increased to 120 volts at 23.5 amperes at the end of two minutes. For the first two minutes there was no indication of a temperature increase in the precoat material. However, from two to four minutes the temperature increase in the precoat material was at a rate of about 3.3°K per minute. At this time the voltage was increased to 140 volts at 26.5 amperes. The temperature increase in the precoat material from four minutes until the time of foaming was at the rate of approximately 10°K per minute. The current being applied to the heating element remained the same until the cool-down portion of the process dictated a decrease in temperature.

Light banks for camera coverage, for which locations are shown on Figure 15, were partially turned on throughout the heat-up period. The effects can be seen in Figures 16 and 17. At a temperature of 344°K there was a temperature spread of about 5.5°K between the lighted side of the experiment and the side directly opposite the lights. However, at this time all lights necessary for movie cameras were turned on and remained on for a period of 10 minutes. These lights still encompassed only a portion of the sphere and therefore left a shaded area on the precoat material. From this time until foaming of the precoat material, temperature spread between the lighted side and shaded side of the precoat material continued to widen.

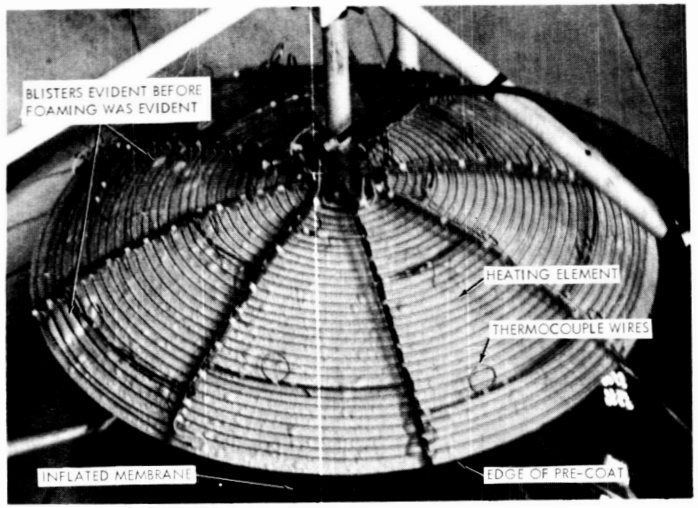

A. Membrane with precoat applied.

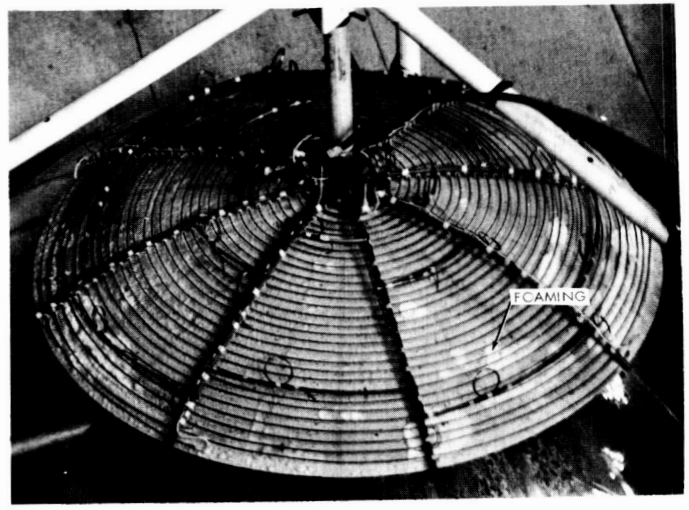

B. First appearance of foaming action.

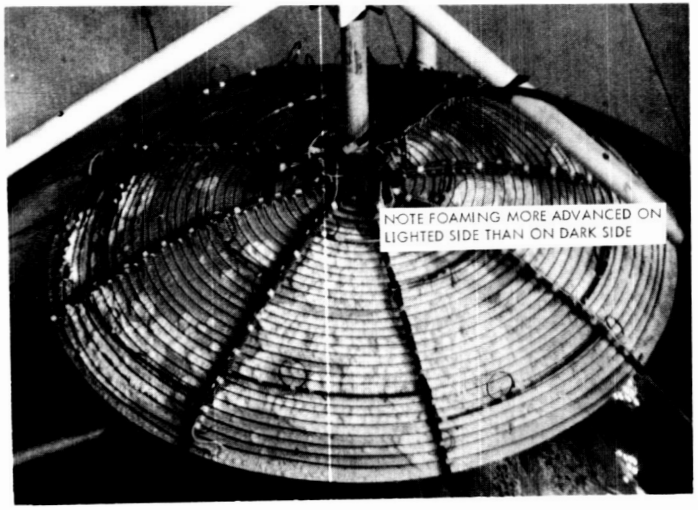

C. Propagation of foaming action.

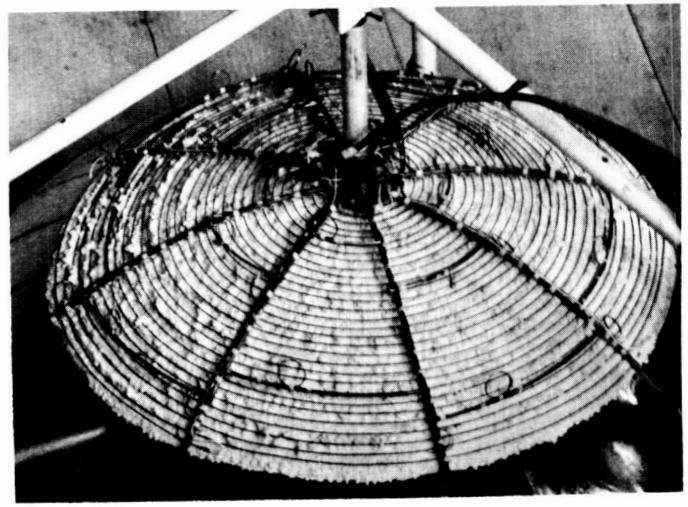

D. Foaming nearing completion.

Figure 16. - Foaming operation - preliminary mirror.

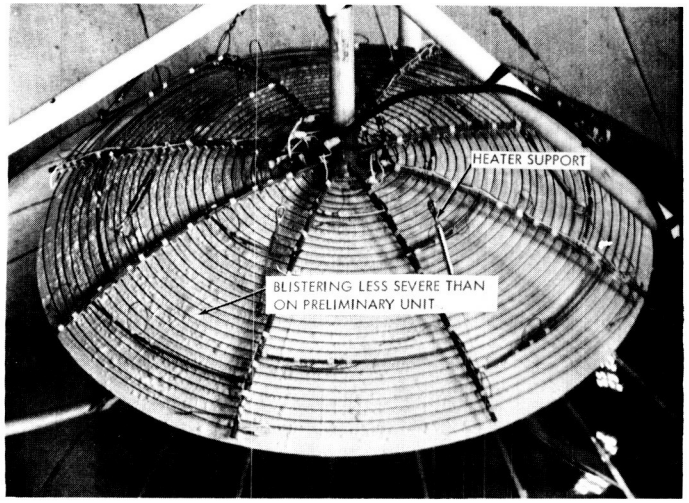

A. Membrane with precoat applied.

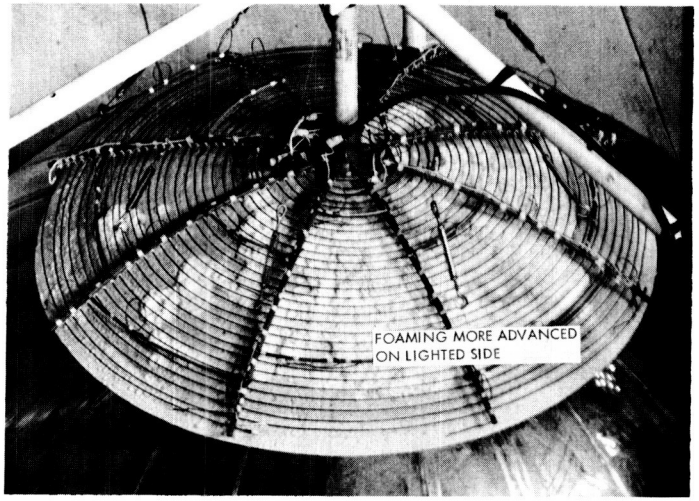

B. Propagation of foaming.

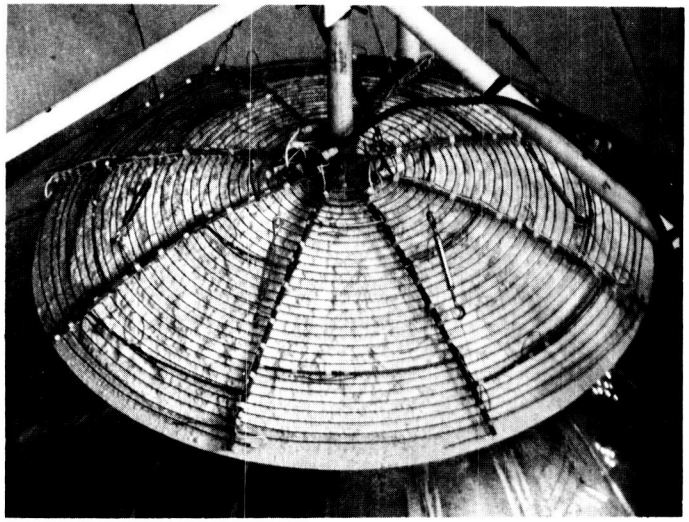

C. Foaming nearing completion.

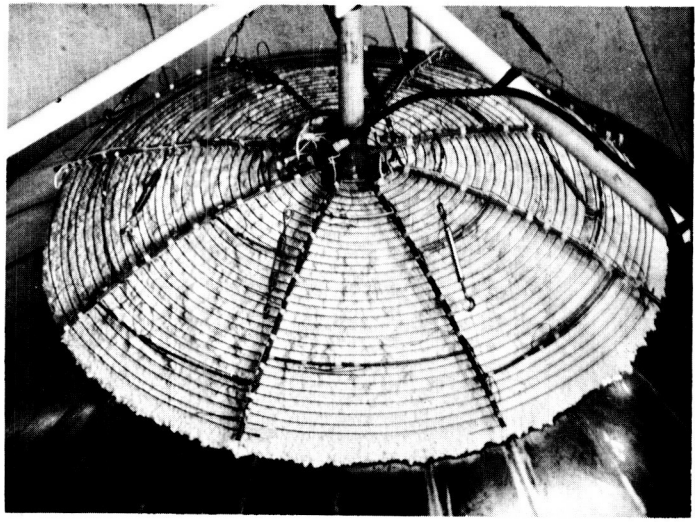

D. Foaming complete.

Figure 17. - Foaming operation - final mirror.

Table V. - 18.29 m sphere pressure-time chart for preliminary mirror.

Time (4-15-66)	Absolute Pressure (N/m^2)	"A" gage (N/m^2)	"B" gage (N/m^2)	"C" gage (N/m^2)	McLeod and/or ionization gage (N/m^2)
3:30 a.m.	59995.08				
4:00	17331.91				
4:30	6666.12				
5:00	3999.67				
5:30	1066.58	1066.58			
6:00		266.64			
6:30		79.99	79.99		
7:00		33.33	33.33		
7:30		22.66	22.66		
8:00		21.33	21.33		
8:30		20.00	20.00		
9:00		20.00	20.00		
9:30		17.33	20.00		
10:00		13.33	20.00		
10:30		13.33	21.33		
11:00		13.33	21.33		
12:00		13.33	14.66		
12:30 p.m.		13.33	10.00		
1:00		13.33	6.00	6.67	
1:30		13.33	3.33	2.80	
2:00		13.33	1.60	0.87	
Prefire					0.09
Post-fire				2.53	

Table VI. - 18.29 m sphere pressure-time chart for final mirror.

Time	Absolute Pressure (N/m^2)	"A" gage, (N/m^2)	"B" gage (N/m^2)	"C" gage (N/m^2)	McLeod and/or ionization gage (N/m^2)
4-19-66					
2:30 p.m.	26664.48				
3:00	10665.79				
3:30	4666.28				
4:00	2666.45				
4:30		599.95			
5:00		133.32			
5:30			33.33		
6:00			14.67		
6:22			11.60		
4-20-66					
7:00 a.m.		266.64	106.66		
7:30		56.00	63.99		
8:00		17.33	20.00		
8:30		12.00	12,00		
9:00		12.00	6.67	7.73	
9:30		5.33	0.80	0.47	
Prefire					0.03
Post-fire				1.80	

On the final mirror the initial temperature of the precoat material was 293°K. From the heating information obtained on the previous unit it was decided to have a pre-zero current applied to the heating element to eliminate the time lag in the first part of the heating cycle. At -1 minute, 120 volts at 23.5 amps were applied to the heating element. At +1/2 minute, the temperature of the precoat material began to increase, and continued to do so at about 3.33°K per minute until +2-1/2 minutes. At this time the voltage was increased to 130 volts at 25.5 amperes. There were no lights on in the vacuum sphere at this time, and the temperature rose at a constant rate of about 8.8°K per minute on all surfaces of the precoat material. At a temperature of 244°K all lights were turned on for the purpose of taking movies. Again a temperature difference was noticeable between the lighted and unlighted sides of the precoat material. However, the spread was not as great as on the earlier unit. The rate of temperature rise increased to about 10°K per minute from this time until foaming. When foaming began, full output of the variac was applied, this being 145 volts at 27.5 amperes. This current was held until cut-back at cool-down. There were 36 thermocouples imbedded in the precoat material. For a comparison of 10 randomly selected thermocouple temperature histories, see Figure 18. Very similar trends were seen on the preliminary unit. It will be noted that thermocouple No. 36 reaches a maximum temperature of only 370°K, whereas the other thermocouples approach 433°K. Thermocouple No. 36 was located so that it touched the hub of the mirror and was retained there by a small patch of precoat material.

At the time foaming began, the temperature of the wire in the heating element had reached 336°K. After full current was applied and the foaming action had occurred, a maximum temperature of 449°K was reached on the heating element wire.

There were no apparent changes in the precoat material during the heat-up process, as can be seen in view A of Figures 16 and 17.

Foam rigidizing process: After reaching foam initiation temperature, the foaming behavior of the precoat was approximately the same for each of the two mirrors and closely paralleled earlier tests of the same precoat formulation. In general, blisters and pimples (such as shown in view A of Figures 16 and 17) visible in the precoat before foaming, had no influence upon the coverage of the membrane by the final foam. However, in the case of one or two blisters, approximately 10 cm across, a bare spot about 0.5 cm in diameter was found after rigidizing, located at about the center of the previous blister.

The larger blisters and pimples that developed in the precoat during the pump-down are believed to have been caused by small amounts of air trapped between the inflated membrane and blocks of precoat as the precoat was applied. Smaller and more numerous pimples in the range of 0.1 to 0.5 cm diameter that developed at the same time are ascribed to (1) acetone dissolved in the precoat, (2) air trapped in the precoat during the pressing into blocks, and

(3) possible slight decomposition of contained azide to produce trapped nitrogen during formulation, pressing, and storage before use.

Qualitatively, there appeared to be fewer ridges in the final foam side surface of the final unit than in the earlier unit. Such ridges seem generally to be produced by intersection of advancing foam fronts. It is believed, therefore, that more nearly uniform heating of the precoat was achieved with the last unit, that larger areas reached initiation at the same time, and that there were fewer major advancing fronts in the course of foaming the whole area (see Figures 16 and 17).

A noticeable contribution to rate of heating the precoat was made by the bank of flood lamps used to illuminate the test assembly. This secondary heating was not uniform over the membrane since the lamp bank was well off the vertical. The effect was reduced in the second experiment by delaying the turning on of illumination until the precoat had reached about 344°K.

Propagation velocity of advancing foam fronts appeared to be largely controlled through the heating of the precoat to initiation temperature by the external radiant heat source. Propagation of the foaming reactions in fact died off in one or two extreme rim areas, receiving only low angle radiation from the primary heating coil. Thermocouple observations over the foamed surface and the sphere pressure-time observations are in agreement that about four minutes elapsed between first and last signals of an exotherm in the second run. In the first run, thermocouples were not quite so close to the rim and the indicated period of foaming was a little shorter.

The time-temperature records (Figure 18) for thermocouples nominally embedded in the precoat before foaming do not generally indicate an exotherm reaching 450°K in either test, but rather peak temperatures of 416 to 433°K. However, 450°K was reached in quality checks of portions of the same batches of precoat used at Langley. The difference is suspected to reside in the use of heavier thermocouple wires (affording larger heat leaks) and a cooler wall around the experiment in the vacuum sphere than in the vacuum bell jar tests previously conducted.

The pressure rise in the sphere during the foaming affords considerable evidence that both the azide rearrangement reaction (liberating nitrogen) and the blocked isocyanate decomposition (liberating phenol) went to virtual completion. Thus in the second test, 0.039 kg N_2, and 0.144 kg phenol should have been released to the vacuum chamber. Assuming an exact 18.29 m diameter evacuated sphere, a final gas temperature of 291°K, and ignoring losses to the pumps, the release of the above amounts of nitrogen and phenol should have resulted in a pressure rise of 1.05 N/m^2 from the nitrogen plus 1.03 N/m^2 from the phenol, or a rise of 2.08 N/m^2. The experimentally observed peak pressure was reported to be 1.80 N/m^2 for the final unit and 2.53 N/m^2 for the other.

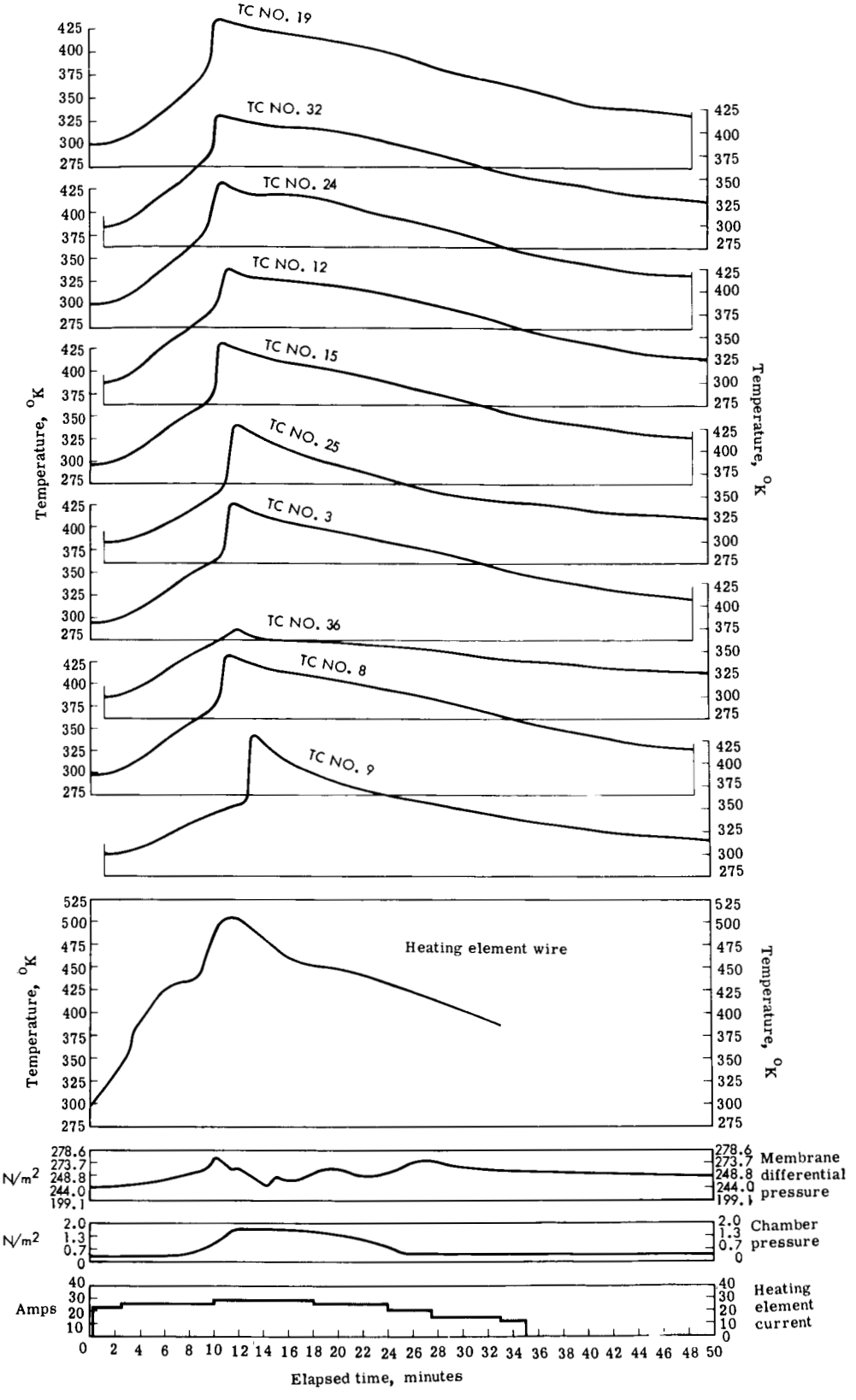

Figure 18. - Temperature and pressure versus time.

Further evidence for completion of the overall foaming reactions is found in determining the hot bar sticking temperatures on the precoat foam. This test was carried out at GAC on trimming from the vacuum formed reflectors. The sticking temperatures were in the usual range of 427 to 436°K.

During the foaming action, the pressure in the mirror membrane increased slightly and was bled off into the vacuum sphere. The foaming differential pressure of 273.7 N/m^2 was maintained fairly closely (see Figure 18).

On the preliminary mirror a thermocouple punctured the mirror membrane and was leaking a small amount of air into the vacuum sphere. However, this puncture hole apparently sealed during the foaming process, because the differential pressure did not indicate additional leaks. This hole is visible in Figure 19.

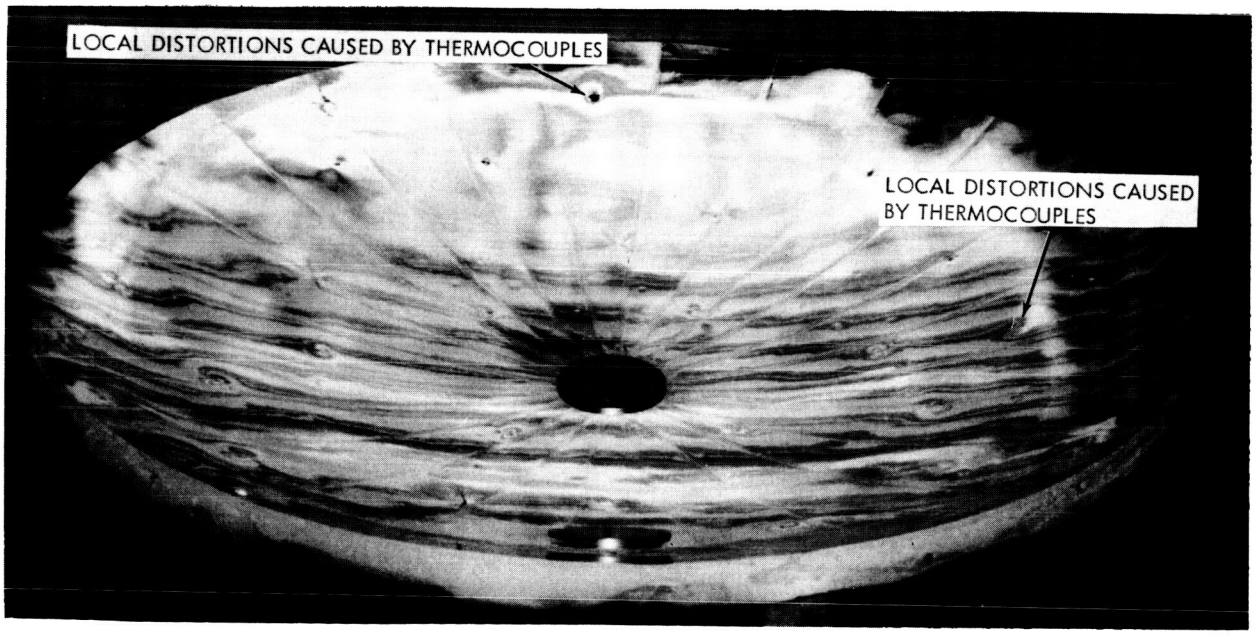

Figure 19. - Preliminary 1.52-meter diameter concentrator.

Cool-down: On both mirrors the cool-down procedure was the same. The heating element was left energized until the heat from the foaming action was dissipated. Then the heating element was shut off in decrements to try to maintain a constant cooling rate. When the foam temperature dropped to about 366°K, the power to the heating element was completely turned off. The foam was then allowed to cool to 316°K before any attempt

was made to release the vacuum in the sphere. The average cooling rate for both mirrors was approximately 2.7°K per minute. For data showing this cool-down for both mirrors, see Figure 18.

During this cool-down period, the vacuum sphere pumps continued to function. At the time of vacuum release, the sphere was registering the same pressure as when the heating of the foam began. The differential pressure of the mirror membrane was maintained between 224 and 273.7 N/m^2 of water during the heat-up, foaming, and cool-down phase of the mirror rigidization.

Vacuum release: For both mirrors the release of the vacuum in the sphere was started when the rigidized foam had cooled to a temperature of 316°K. To keep the rigidized mirror from collapsing, it was necessary to keep a positive pressure inside the rigidized membrane at all times during the vacuum release. The procedure was the same for both mirrors.

The low pressure regulator shut-off valve was closed. A shop air pressure line was attached to the high pressure regulator of the pressure regulation system. This regulator was opened to supply atmospheric pressure on the low pressure regulator shut-off valve. All pumps of the sphere pumping system were stopped. The vacuum release valve of the sphere was opened a very small amount. At the same time the low pressure regulator shut-off valve of the pressure regulation system was opened. The low pressure regulator was adjusted to bleed a small amount of air into the rigidized membrane, maintaining a differential pressure of 248.8 N/m^2. Air was bled in at this rate until the vacuum sphere had reached a pressure of 20.00 N/m^2. At this pressure the vacuum release valve of the sphere and the low pressure regulator of the pressure regulation system were opened more to increase the air flow in both the sphere and the rigidized mirror. The mirror membrane hanging below the clamp band of the sphere was used as a guide. Air flow into the sphere was increased until the air motion inside the sphere caused considerable turbulent motion of the membrane skirt. The low pressure regulator maintained a positive pressure in the rigidized mirror. When motion of the membrane skirt ceased, the rate of air being bled in was increased. When the vacuum sphere reached a pressure of about 46660.8 N/m^2 the vacuum release valve of the sphere was completely open. As the vacuum sphere approached ambient pressure, the low pressure regulator was slowly closed to maintain a 248.8 N/m^2 differential pressure when the vacuum sphere did reach ambient pressure. There were no apparent high pressure surges, either positive or negative, on the mirror membrane during the complete process of releasing the vacuum.

Post vacuum operations. - When rigidization was completed, the 1.52-meter diameter mirrors had to be inspected and evaluated. To do this, steps were taken to maintain the mirror in its rigidized form for evaluation. (Unless otherwise noted, the tasks were performed in the same manner on the preliminary mirror as on the final unit.)

When the sphere pressure had reached ambient, the units were closely inspected. It was clearly noticeable on the preliminary unit that the foam had actually encapsulated parts of the heating element (see view D, Figure 16). This occurred at the outer radii of the mirror where the heating element was closer to the membrane. This did not occur on the final mirror, in which case the heating element was further away from the membrane.

The ring torus backup structure, constructed in halves, was put in place and assembled with nuts and bolts. It was cleaned with MEK solvent and positioned against the back of the solar concentrator (see Figure 20).

This ring torus was located and held in place vertically by adjustable rods suspended from the basic structure. These rods were adjusted horizontally by tying to the frame with lacing cord.

A channel consisting of cardboard and masking tape was built up around the ring torus, leaving space for the bonding foam. The bonding foam was then prepared in accordance with the formulation listed in the paragraph entitled "Bonding of aluminum backup structure to predistributed foam surface," page 13.

After 20 seconds of mixing with a high-speed impeller, the material was poured into the channel formed on the back of the solar concentrator. It began to rise and foam almost immediately. Several mixes were required to completely embed the torus ring.

The foam was allowed to cure. It experienced a temperature variation from 289 to 297°K for 17 hours. Heat was then applied with a heat gun and the foam was exposed to a temperature of 305 to 325°K for a period of two hours. The membrane remained pressurized throughout this process to 27[illegible] N/m². The solar concentrator was then trimmed to the 1.52 m diameter.

The pressure was then released and the mirror placed on a temporary wooden support in preparation to finish trimming the periphery. It is shown in this position in Figure 21.

The final mirror reflecting surface can be seen in Figure 22. A measurable improvement was achieved beyond that of the preliminary mirror, Figure 19.

Log of operations. - Table VII is a log of the operations carried out from the setup in the vacuum sphere to the completion of each unit through attachment of backup structure.

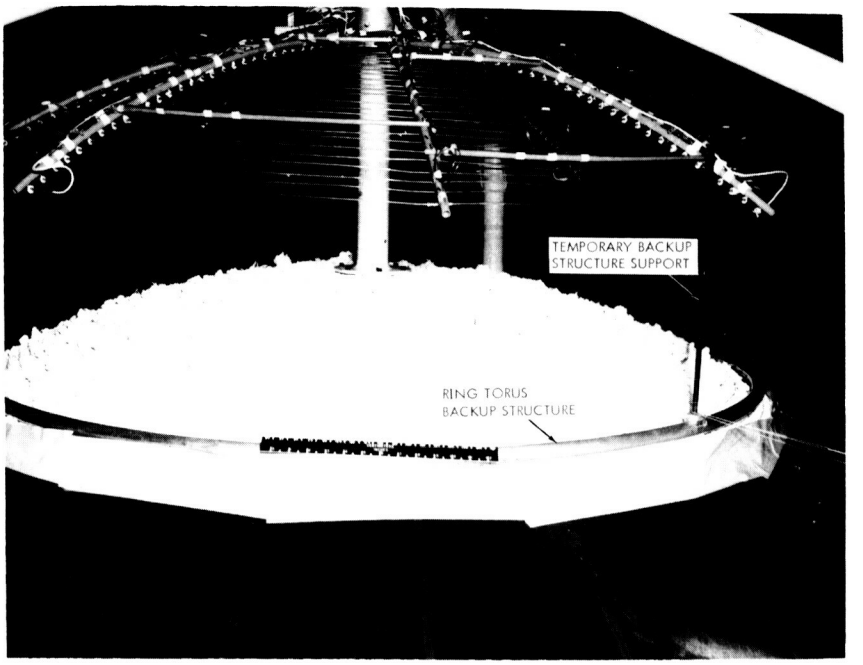

Figure 20. - Preparations for backup structure attachment.

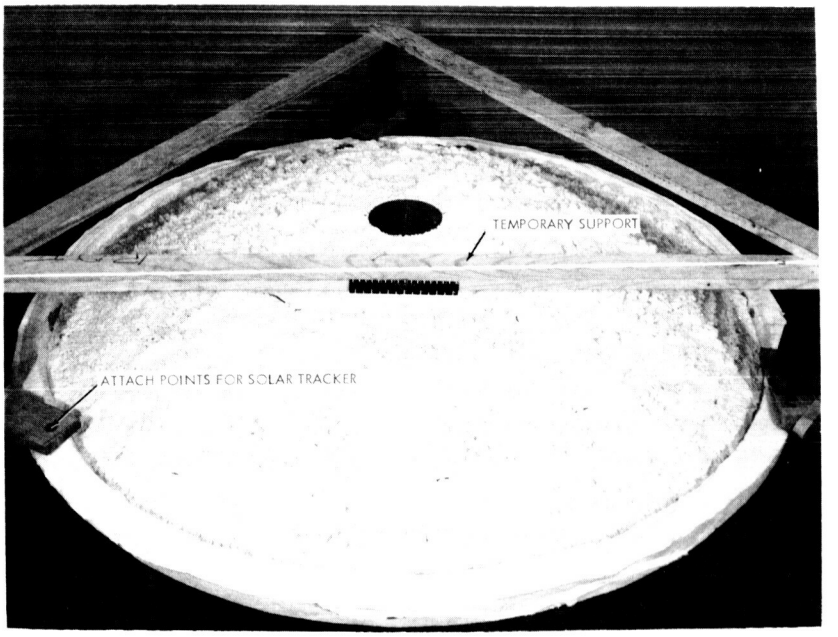

Figure 21. - Final mirror with backup ring attached.

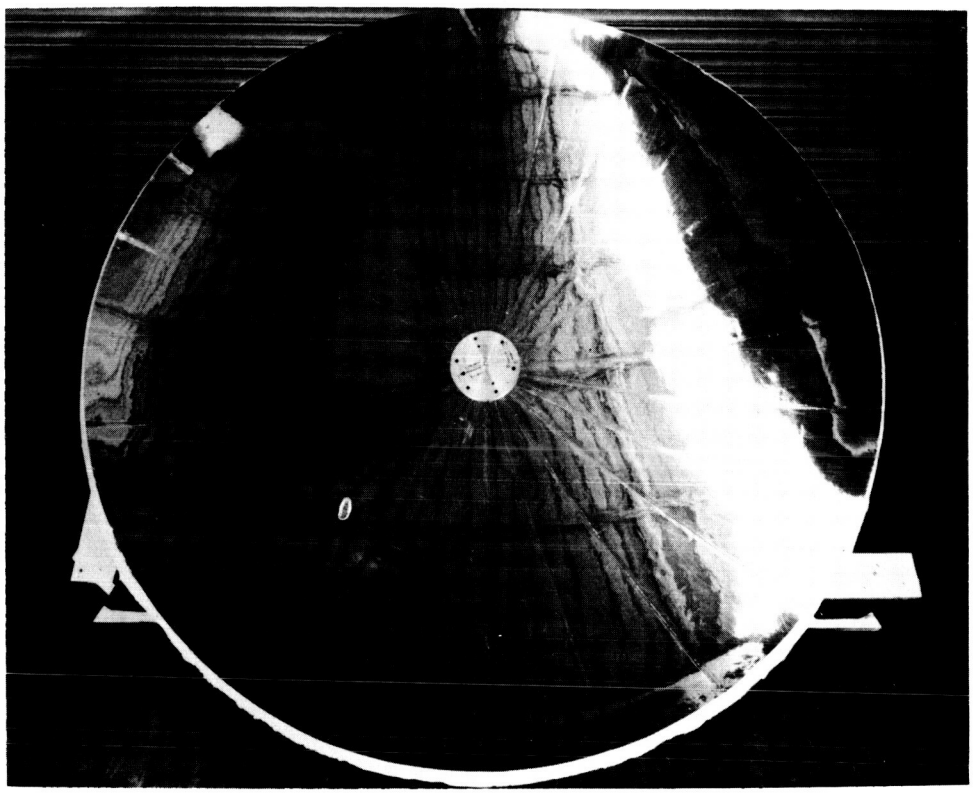

Figure 22. - Final mirror.

Evaluation of Reflector Rigidization

The materials, processes, techniques and test fixtures developed, and fabricated during the course of this program were all utilized to rigidize two reflectors in the 18.29 m vacuum chamber. The results of the work accomplished are evident when evaluating the reflectors produced. Evaluation is made of the process used, the concentrator shape and reflecting surface quality.

Processes. - The concentrator rigidization runs afforded the final tests of the reproducibility of the foaming process and resultant foam. The heating schedule brought on initiation of foaming at the expected temperature level of the precoat (generally 355 to 360°K) and the foaming reaction propagated through the entire precoat. The physical structure and thickness of the resultant foam, its state of chemical cure, and strong bonding of foam to envelope, all reproduced results close to those obtained 18 or more months earlier with replicate batches of precoat based on Formulation No. 394-91.

The present runs were carried out at a higher average vacuum (by about one order of magnitude) than prevailed in any previous rigidization tests.

Table VII. - Log of operations.

Operation	Reflector	
	Preliminary	Final
Weight of precoat applied to membrane, kg	1.435	1.481
Time required for precoat application, hr	1.2	0.7
Ambient temperature during precoat application, °K	290	294
Location of heater:		
Height above membrane at hub, cm	5.0	5.0
Height above membrane at rim, cm	2.5	5.0
Extension of precoat beyond outermost coil of heater, cm	5.1	3.0
Time required for heater, thermocouple, and other installation and adjustments and contour check-out, hr	2.0	0.75
Elapsed time from precoat application to start of sphere pump-down, hr	11	1.5
Elapsed time from start of pump-down to start of foaming process, hr	10	17
Time on diffusion pumps before start of foaming process, hr	2 - 4*	~2
Elapsed time from heat application to foam initiation - minutes	9.5	12.0
Elapsed time of foaming process - minutes	3.5	4.0
Cool down time from foaming completion till chamber pressurization - minutes	34	36
Pressurization of chamber - hrs	3.2	2.6
Elapsed time from chamber pressurization to application of backup structure - hrs	1.5	0.8
Cure time of backup structure foam - hrs	64	14
Backup structure cure temperature °K	293	10 hrs at 296 4 hrs at 320
Maximum temperature during foam process average °K	416	433

* Leaks were encountered.

This did not in any way affect the performance of the precoat material. Therefore, there is no evident reason to expect any change in foaming behavior as a result of the vacuum of space.

Each of the present runs represented a scale-up of 6X in area rigidized over the largest prior tests and 12X in area rigidized with sheeted precoat. There was also a scale-up of 10X over past work in the preparation of prepolymer used in formulating precoat for the present tests.

A solid demonstration of the storage stability of precoat material was afforded by use of 15 day-old material for the first test and 34 day-old material for the second.

Concentrator Shape. - The contours of the test articles were determined through the use of the contour measuring tool as described previously in the fabrication section of this report. This device measured the deviation of the actual parabolic contour from that of the desired contour. The details of operation of this tool were discussed in the report.

Contour measurements were made by rotating the measuring aim through 360°, at the following intervals in the rigidization process:

Run No.	Rigidizing Stage
1.	Membrane pressurized in atmosphere
2.	Membrane pressurized in evacuated environment
3.	For the preliminary model reflector - At maximum foam temperature while foaming was taking place. For the final unit - After the foaming process was completed and a slight decrease in temperature was indicated.
4.	During cooling process, temperature $\approx$ 366° K
5.	After equalization of sphere pressure (atmospheric)
6.	After applications of backup structure

This procedure enabled all important changes in contour to be recorded.

After completion of the preliminary unit, the data was tabulated to find the deviations of the reflector at the various radii. Runs No. 1, 3, and 6 were compared to establish the movement of the mirror during the foaming process. From this tabulated data, it was determined that the finished reflector had a maximum deviation from nominal at the 76.2 cm radius at an angular rotation of 315°. Angular rotation of the contour measuring arm always starts at a predetermined 0° position. When the rotation is in the opposite directions, all readings are translated to their proper location. The deviation at this point was 1.13 cm. During

the foaming process when maximum temperature was realized due to exotherm, the deviation of this point exceeded the measuring capabilities of the instrumentation. From the total of the tabulated data, 56.88 percent of the reflector had a deflection of less than ± 0.5 cm. Table VIII lists the percentage deviation less than ± 0.5 cm at the various radii of the preliminary mirror.

Table VIII. Percent Deviation less than 0.50 CM at Various Radii for the Preliminary Mirror

Radius cm	% Deviation less than 0.5 cm	Radius cm	% Deviation less than 0.5
12.7	100	58.42	38
30.48	100	64.77	0
41.91	100	71.12	63
50.8	46	76.20	8

From this same data it is evident that the first unit had a deflection of less than 0.25 cm for less than 30 percent of the surface.

On the basis of this information, appropriate adjustments were made to the alignment structure to provide an improved contour for the final mirror. These changes were effective and a more accurate mirror resulted.

For the final mirror, runs No. 3 and No. 6 were plotted on a polar graph (see Figure 23). Cross sections of the paraboloid were also plotted for runs No. 1, No. 3 and No. 6, at all measured radii and at various angular degrees as indicated in Figure 24 - the first radius being arbitrarily placed outside the hub of the reflector and the remaining radii so calculated to divide the remainder of the reflector into equal areas.

For the completed final mirror, it will be noted from the polar plot (Figure 23) that the maximum deviation of +0.4 cm, from the theoretical reflector, was located at a radius of 67.88 cm and an angular rotation of 75°. During the foaming process, a maximum deviation of +1.04 cm was witnessed at this same point. The reduced data shows that 81 percent of the completed final concentrator had a deviation, from theoretical, of less than ± 0.25 cm.

Table IX gives the percent of the completed final mirror at various radii with a deviation of less than 0.25 cm.

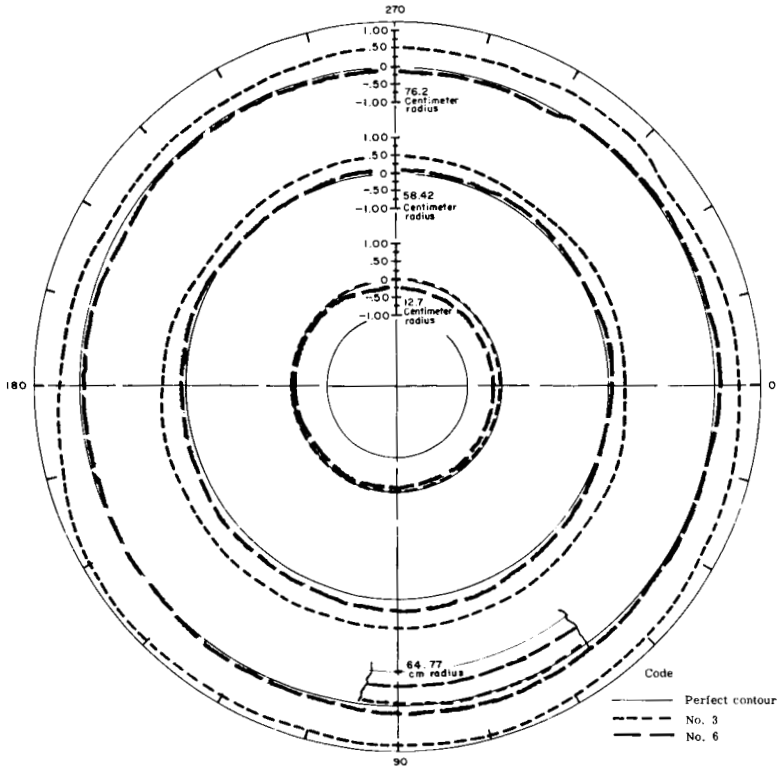

Figure 23. - Polar graph - final mirror.

Table IX. - Percent deviation less than 0.25 CM at various radii for the final mirror.

Radius (cm)	Percent Deviation Less Than 0.25 cm	Radius (cm)	Percent Deviation Less Than 0.25 cm
12.7	63	58.42	88
30.48	58	64.77	75
41.91	88	71.12	96
50.8	88	76.2	92

It will be noted in Figure 24 that at 0, 45, and 90 degrees there is a definite reverse to the contour deviation between a radius of 71.12 cm and 76.2 cm. This includes the 75° angular location of maximum deviation. The section between 0 and 120° was the last area in which the backup structure foam was applied. From the way that the outer area of the mirror is contoured between 0 and 120°, it appears that the backup structure foam has twisted this portion of the concentrator.

In all cases, a plus (+) deviation indicates a deviation that is outside the contour of the desired parabolic contour, and a minus (-) deviation indicates a deviation that is inside the desired parabolic contour (see Figure 25).

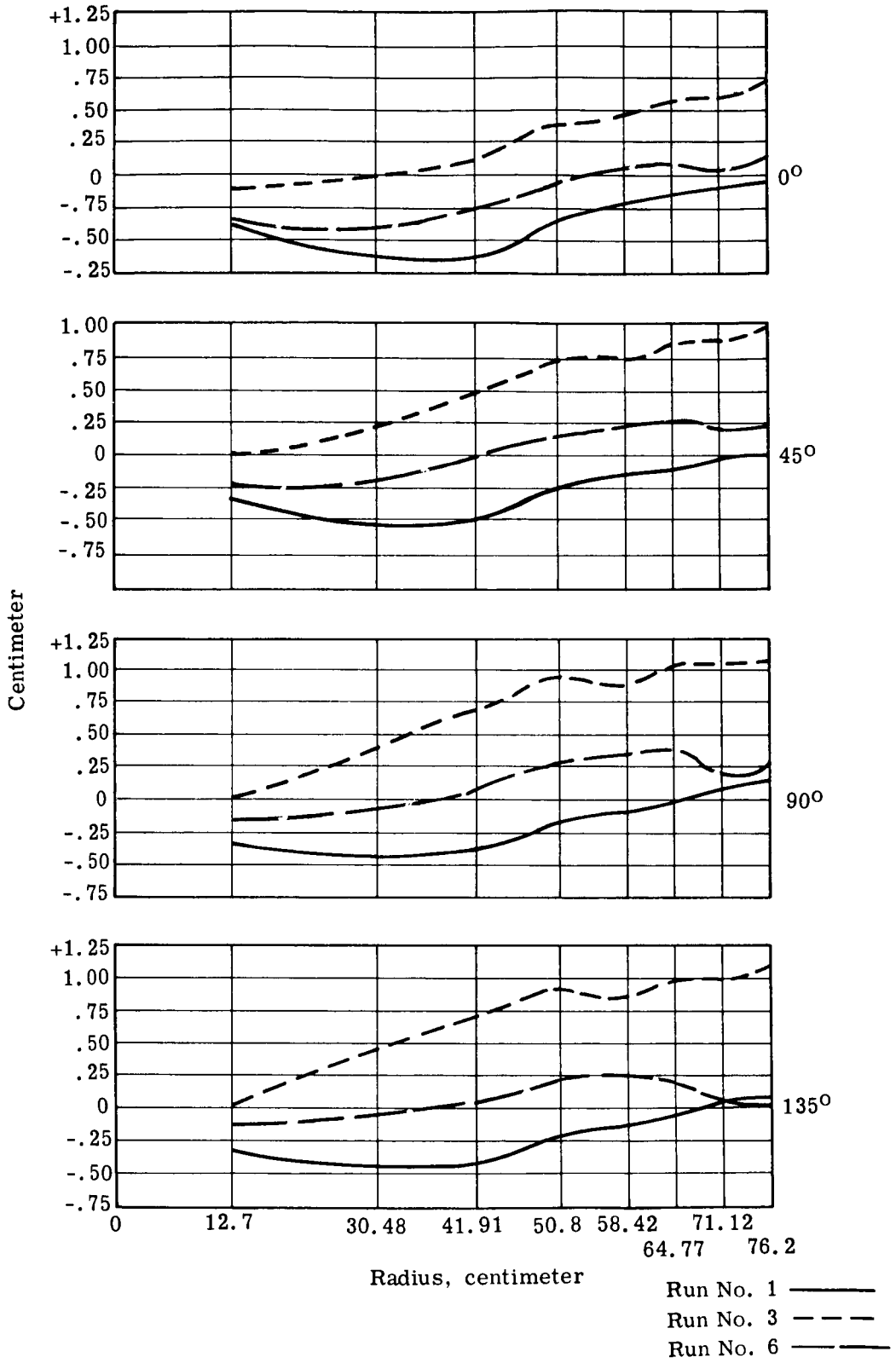

Figure 24 (Sheet 1). - Sections of polar plot - final mirror.

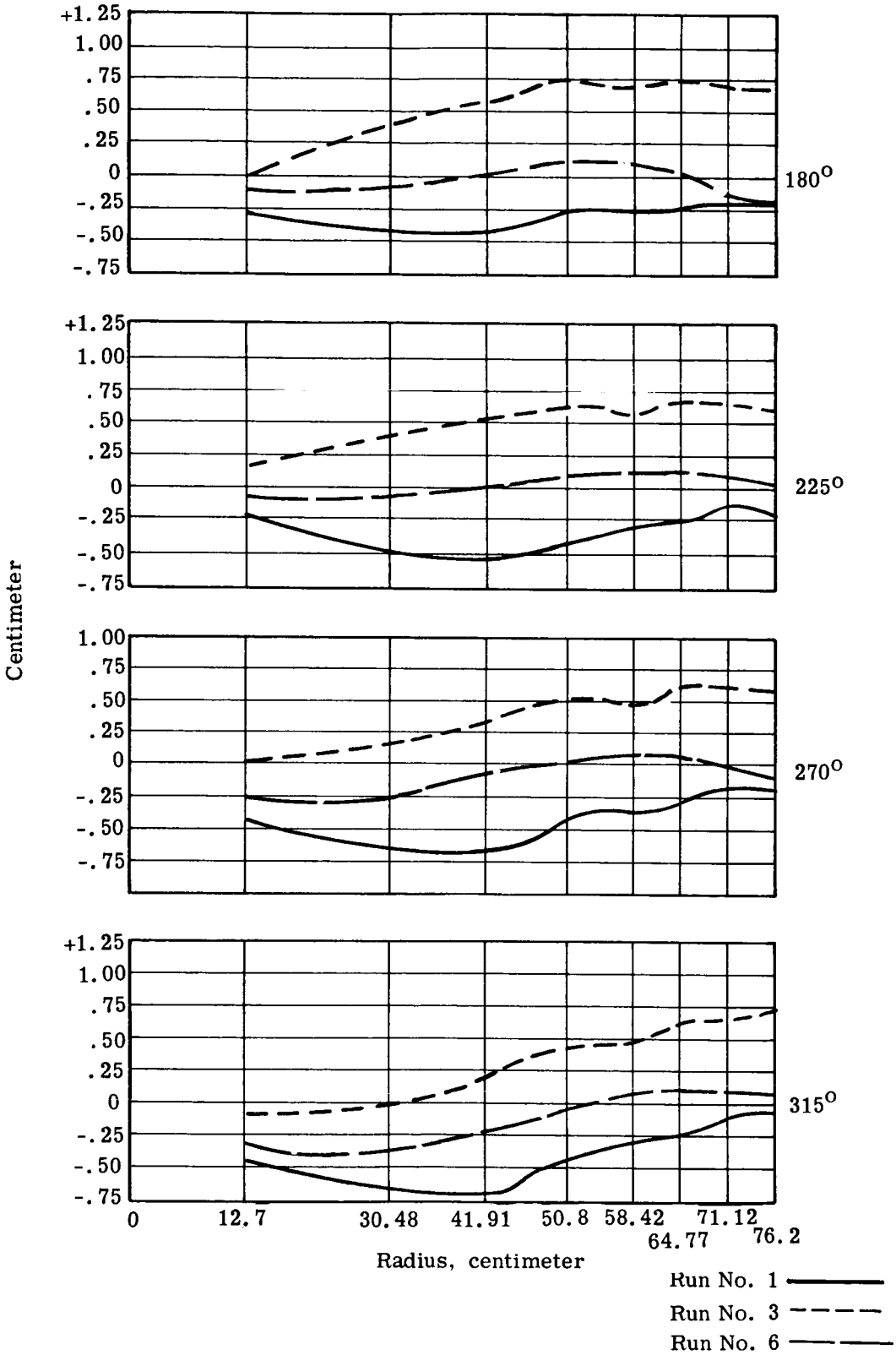

Figure 24 (Sheet 2). - Sections of polar plot - final mirror.

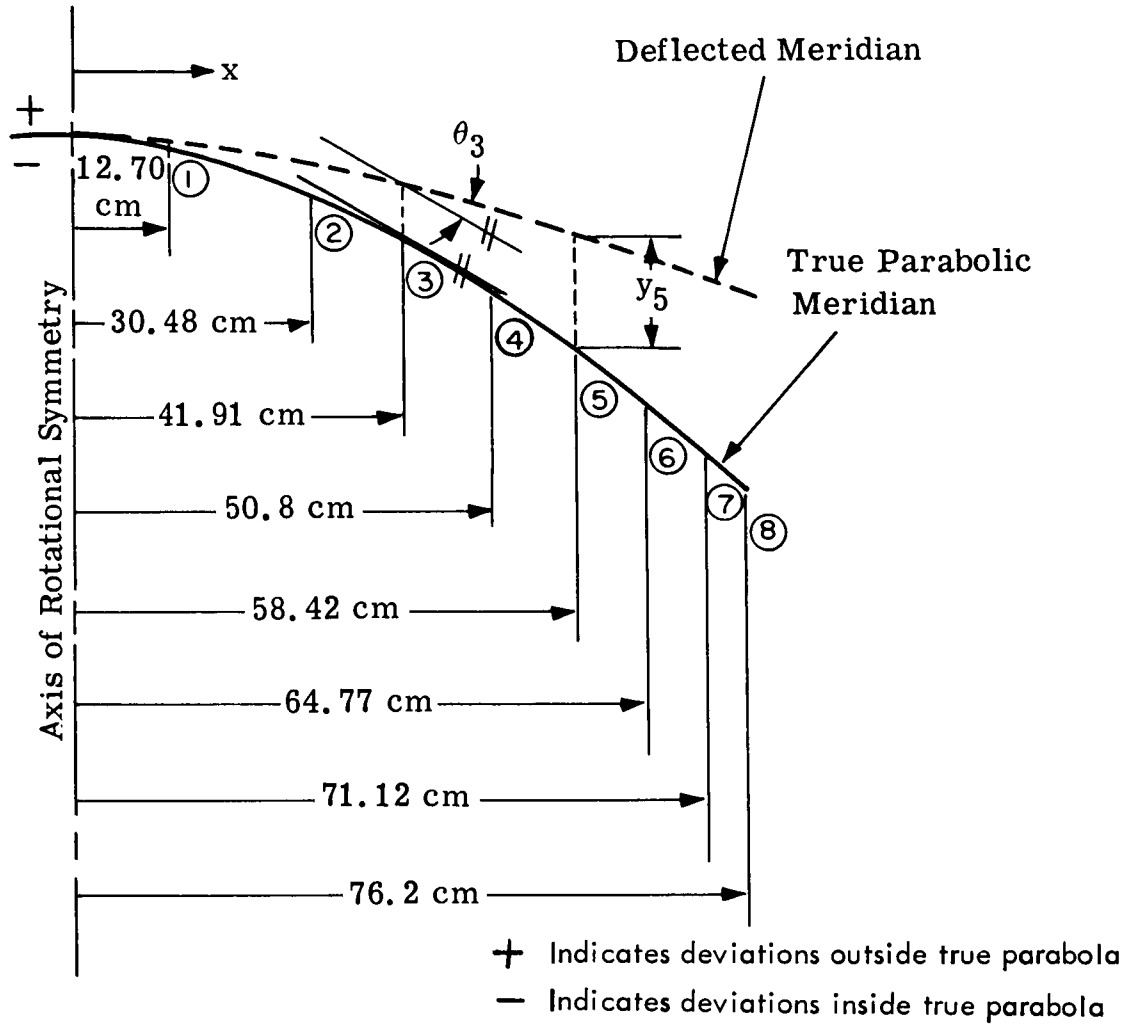

Figure 25. - Deflected and undeflected half-meridian.

In evaluating the reflector, the deviation of points on a radius is used to determine the change of the focal point of the concentrator. Generally speaking, it can be said that a plus point will extend the focal point, and a negative point will retract the focal point. However, this is only true when considering a single point, and in this case the interest is in the total surface of the concentrator. Therefore, the interest is in the difference of changes in deflection from point to point or the angular deviation. To illustrate this, see area C of Figure 26 and Run 6 at 180° of Figure 24. The deflection at radius 50.80 is +0.1 cm greater than the deflection at the 41.91 cm radius. This area is then progressively positive and will cause an extended focal point.

The concentrator deviation measurements were made at eight points along the half meridian of the paraboloid and in a direction that was parallel to the rotational axis of symmetry as shown in Figure 25. A numerical scheme for converting these measurements to the corresponding angular deviations is developed herein.

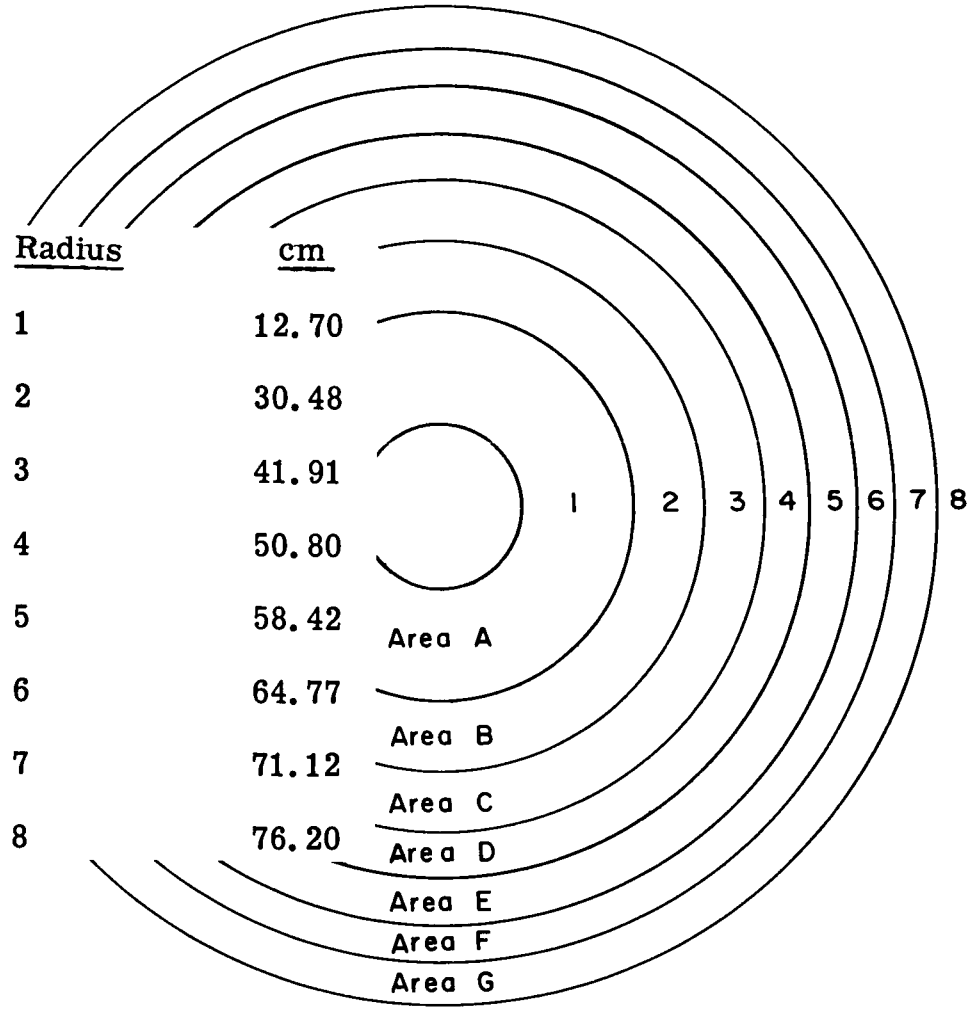

Figure 26. - Reflective areas of final mirror.

This analysis gives angular deflections that are greater than the actual deflections that exist. Consider the deflection of point i, Figure 27. Because deflections were taken parallel to the axis of symmetry, the analysis is based on Figure 27 (a) rather than the more accurate approximation indicated by Figure 27 (b). The deflection, θ_i, will be slightly larger than θ_i' since, at each point as seen in Figure 27, $\Delta s > \Delta x$ and $y > \mathcal{E}$.

The numerical scheme for determining the slope, $y_i' = \tan \theta_i$, at the intermediate pivotal points is given by equation 2.3.4 of reference 1 with the nomenclature of Figure 28 (a). This is directly applicable to point 1 of Figure 25. However, since points 2 through 7 correspond to Figure 28 (b), a similar equation must be derived. This was done and is given here as equation (3).

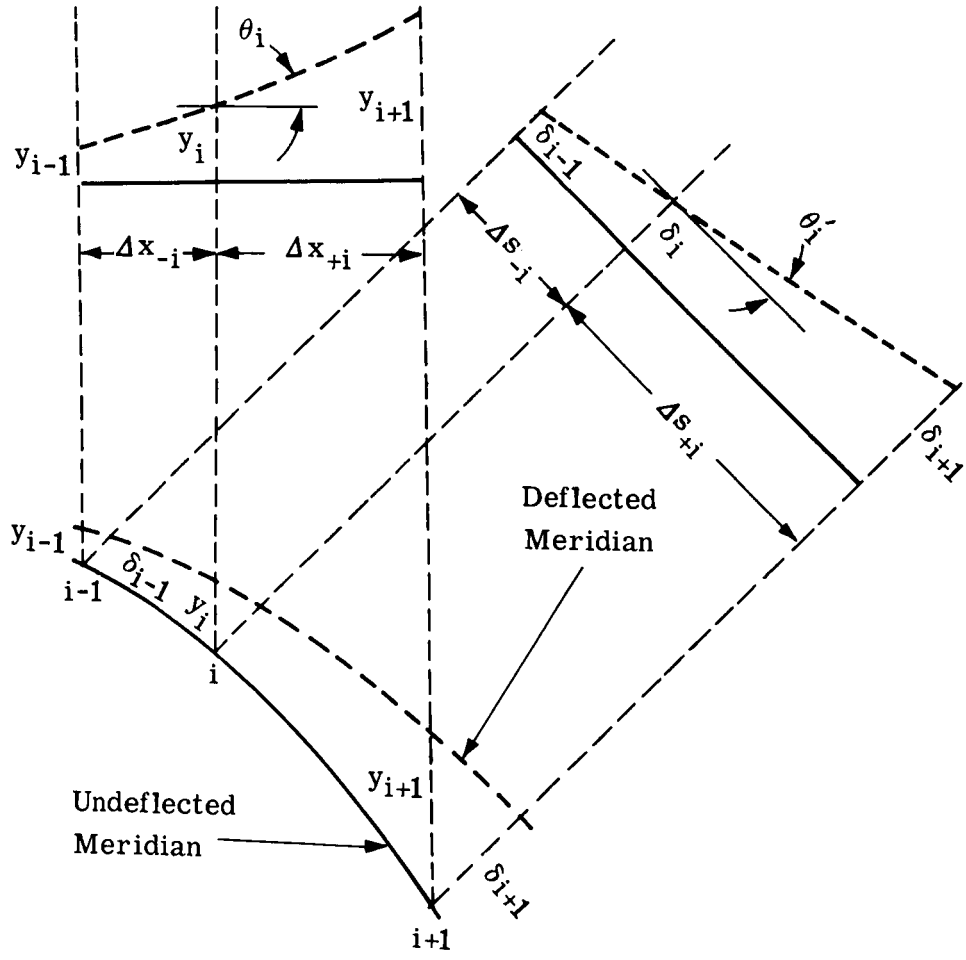

Figure 27. - Basis of the approximate angular deflections.

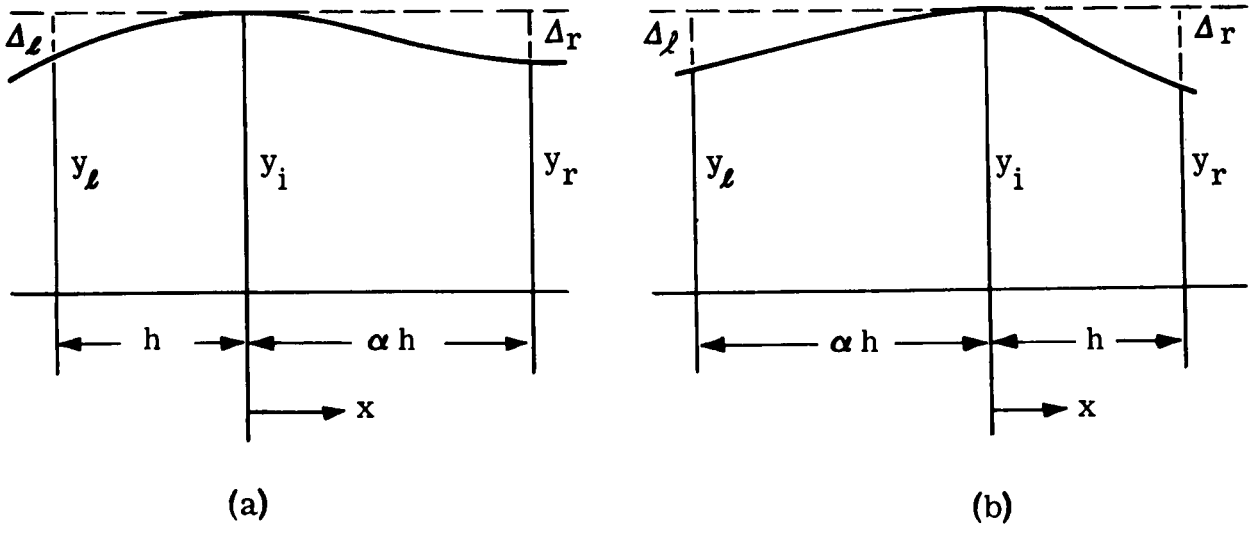

Figure 28. - Two cases of unequally spaced pivotal points.

For the case of Figure 28 (a), (eq 2.3.4, ref. 1)

$$y_i' = \frac{1}{\alpha(\alpha+1)h} \left[y_r - (1-\alpha^2)\, y_i - \alpha^2 y_\ell\right] \tag{1}$$

or, from Figure 25,

$$y_i' = \frac{1}{\alpha(\alpha+1)h} (\alpha^2 \Delta_\ell - \Delta_r) \tag{2}$$

for the case of Figure 28 (b)

$$y_i' = \frac{1}{\alpha(\alpha+1)h} \left[y_\ell - (1-\alpha^2) y_i - \alpha^2 y_r\right] \tag{3}$$

or

$$y_i' = \frac{1}{\alpha(\alpha+1)h} (\alpha^2 \Delta_r - \Delta_\ell) \tag{4}$$

The end point, 8, is unique in that an extrapolation technique must be used to determine the slope. Such a formula, based on a three-point interpolation Lagrangian formula, is given by equation 3.8.3 of reference 2. However, this is valid for equally spaced pivotal points. Its use here is considered to be an adequate approximation, since the spacing of points 6, 7, and 8 deviates by only 11 percent from the average.

By equation 3.8.3 of reference 2,

$$y_r' = \frac{1}{2h_e} (3y_r - 4y_i + y_\ell) \tag{5}$$

where an average pivotal point spacing must be substituted for h_e so that

$$y_r' \approx \frac{1}{(1+\alpha)h} (3y_r - 4y_i + y_\ell) \tag{6}$$

or, from Figure 26,

$$y_r' \approx -\frac{1}{(1+\alpha)h} (3\Delta_r + \Delta_\ell) \tag{7}$$

The following set of equations for the slope at each of the eight points was obtained by substituting the proper values of α and h, as obtained by the dimensions of Figure 25, into equations (3), (4), and (7).

REFERENCES

1. Salvadori, M.G. and Baron, M.L., Numerical Methods in Engineering. Prentice-Hall, Inc., New York, 1952.
2. Hildebrand, F.B., Introduction to Numerical Analysis. McGraw-Hill Book Company, Inc., New York 1956.

Point	Slope Equation
1	$y_1' = 0.022176\ (\Delta_2)$
2	$y_2' = 0.020335\ (2.79391\ \Delta_3 - \Delta_1)$
3	$y_3' = 0.040019\ (1.61036\ \Delta_4 - \Delta_2)$
4	$y_4' = 0.053030\ (1.37569\ \Delta_5 - \Delta_3)$
5	$y_5' = 0.063503\ (1.27284\ \Delta_6 - \Delta_4)$
6	$y_6' = 0.072506\ (1.21462\ \Delta_7 - \Delta_5)$
7	$y_7' = 0.080586\ (1.17614\ \Delta_8 - \Delta_6)$
8	$y_8' = 0.087395\ (3\Delta_8 + \Delta_6)$

The slope equations of these points depict the angular deflection in a single plane passing through the axis of rotational symmetry. They do not take into consideration the compounding effect created by the change in slope from one plane to another as you rotate around the axis of symmetry.

Based on the above equations, we find that points 2 through 7 inclusive each contain two equal areas of the mirror, whereas those for points 1 and 8 use estrapolated values. Considering only those points that cover actual areas of the concentrator, we find that 31.2 percent of the preliminary concentrator has a tangential angular deflection of less than ± 0.5°. The maximum deflection of any point is 1.8°. For a breakdown of the angular deflection, of the preliminary mirror, see Table X.

Table X. - Angular deviation of specific areas-preliminary mirror.

Point	Areas Included (See Figure 26)	Max Angular Deflection (Degrees)	Deviation Less Than 0.5° (Percent)
2	A & B	1.09	0
3	B & C	1.56	0
4	C & D	1.4	25
5	D & E	1.05	29.1
6	E & F	1.05	87.5
7	F & G	1.80	45.8

For the final concentrator, considering only those points that cover actual areas of the concentrator, it is found that 47.9 percent of the concentrator has a tangential angular deflection of less than ± 0.5°. The maximum angular deflection of any point is 1.31°. The portion of the concentrator showing an angular deflection of greater than 0.5° was located angularly between 75 and 165°. This is the same mirror area having maximum deflection and bad edge reverse curvature. For a breakdown of the angular deflection of the final mirrors, see Table XI.

Table XI. - Angular deviation of specific areas-final mirror.

Point	Areas Included (See Figure 26)	Max Angular Deflection (Degrees)	Deviation Less Than 0.5° (Percent)
2	A & B	0.75	79.2
3	B & C	1.31	4.2
4	C & D	1.29	29.2
5	D & E	0.65	79.2
6	E & F	1.24	62.5
7	F & G	1.27	33.3

Figure 29 is a comparison of the final finished mirror at all radii, through a full 360° sweep. This figure shows the difference in deviation of the mirror membrane at atmospheric conditions and in the vacuum sphere at a pressure of less than 0.13 N/m^2. In both cases a differential pressure of 273.7 N/m^2 was applied to the mirror membrane. The entire parabolic shape opened up with respect to the initial setting. The largest displacement was .635 cm at an angular location of 75° and at a radius of 76.2 cm.

For a complete history of the changes at a specific radius of 76.2 cm, see Figure 30. This shows the movement of this LVDT through the full 360° sweep for all six sweeps involved in the foaming process. It can easily be seen how the parabolic contour moves outside the theoretical contour through the pump-down and foaming process, and how this movement is reversed through the cooling process and by releasing the vacuum in the sphere. There are very definite movements of the mirror membrane through all of these phases.

To compare these movements for the full concentrator rather than one radius, see Figure 31. This shows measurements No. 1, 3, and 6. That is, the initial setting of the membrane, its maximum expansion during foaming, and the final configuration after cool-down and application of backup structure. It can be seen that it is necessary

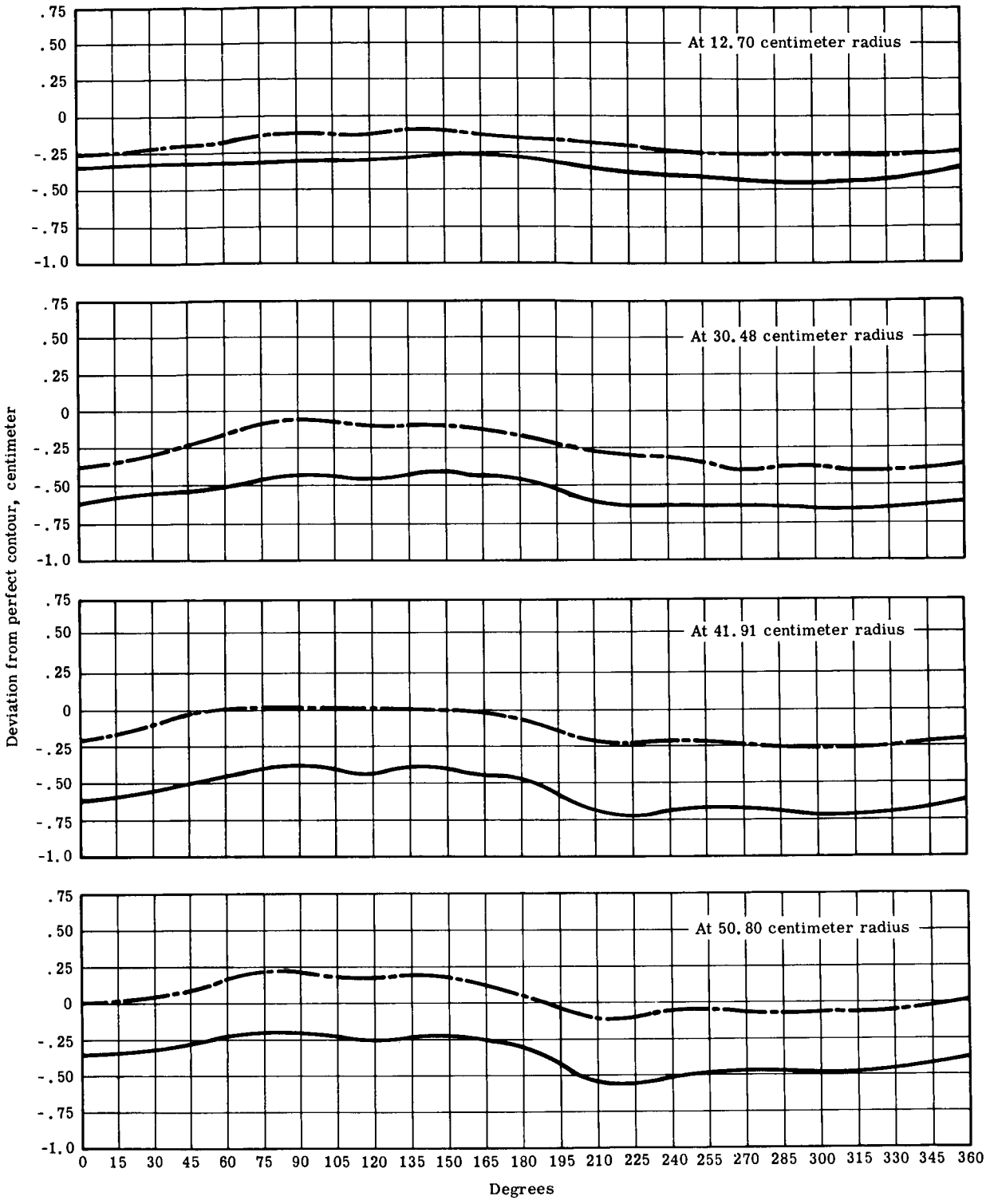

Figure 29 (Sheet 1). - Contour comparison of membrane from all stations in atmosphere and in vacuum - final mirror.

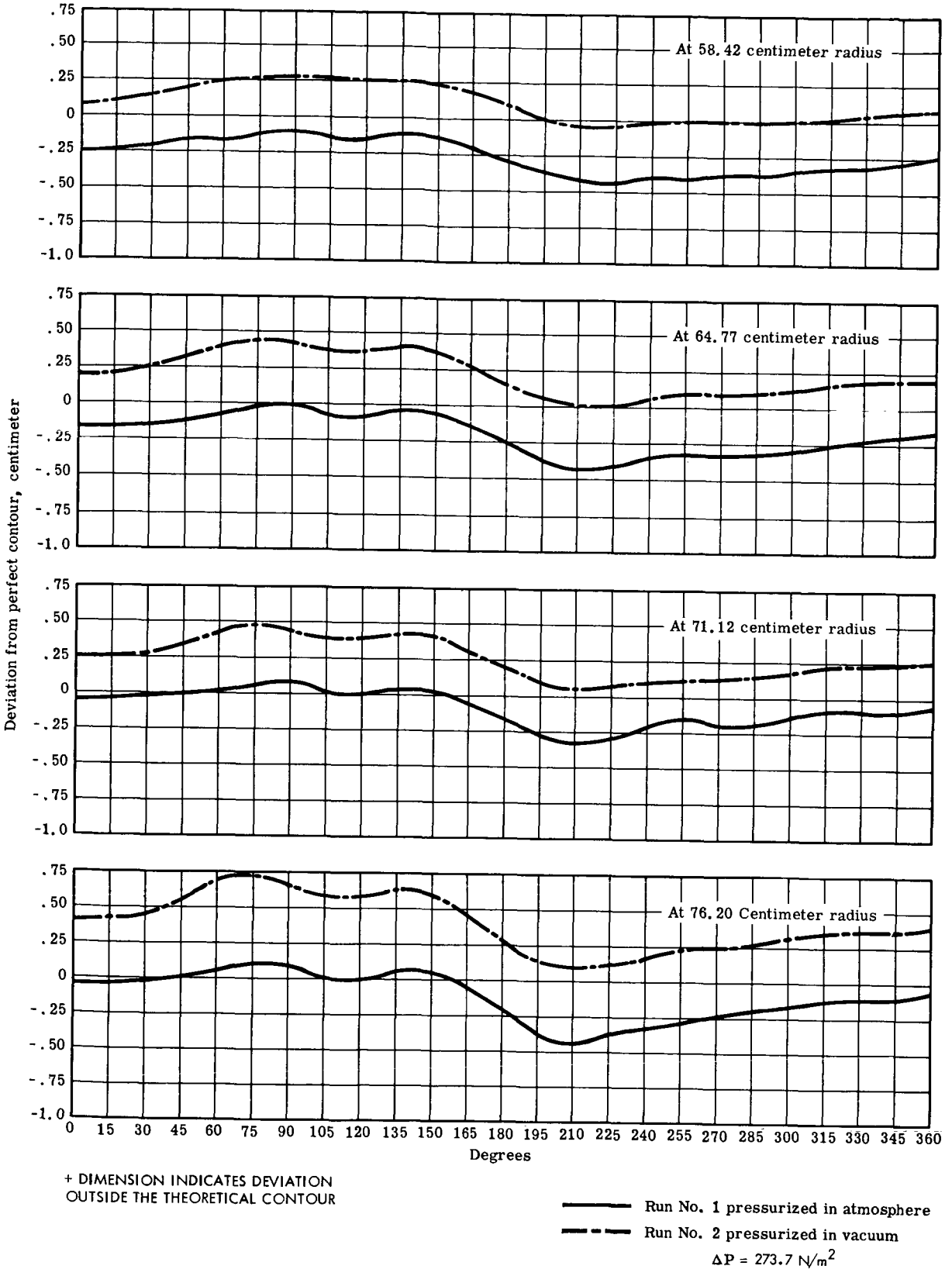

Figure 29 (Sheet 2).- Contour comparison of membrane from all stations in atmosphere and in vacuum - final mirror.

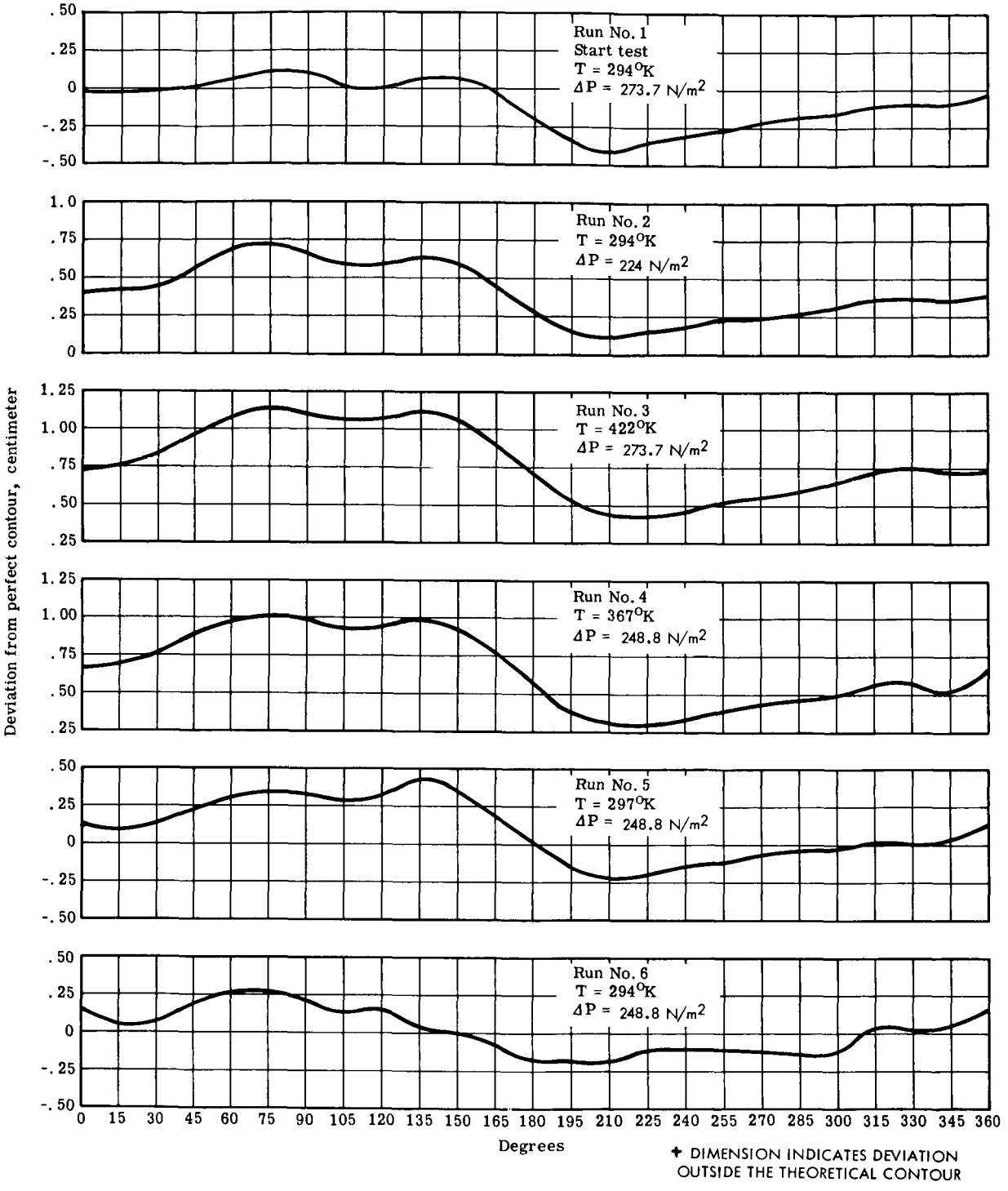

Figure 30. - Contour comparisons of all runs from one station (78.2 cm radius) - final mirror

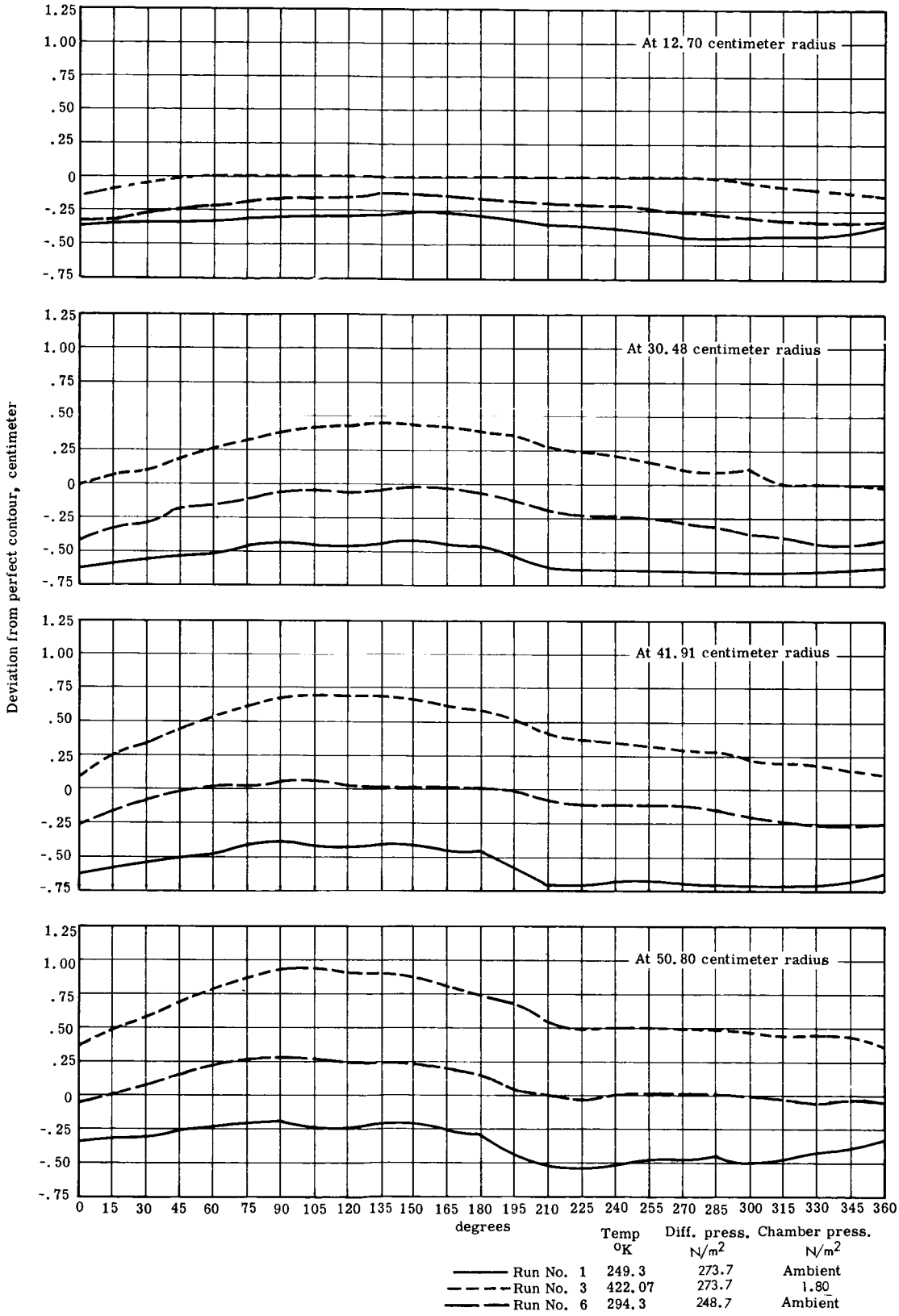

Figure 31 (Sheet 1). - Contour comparisons from all stations before, during, and after application of backup structure - final mirror.

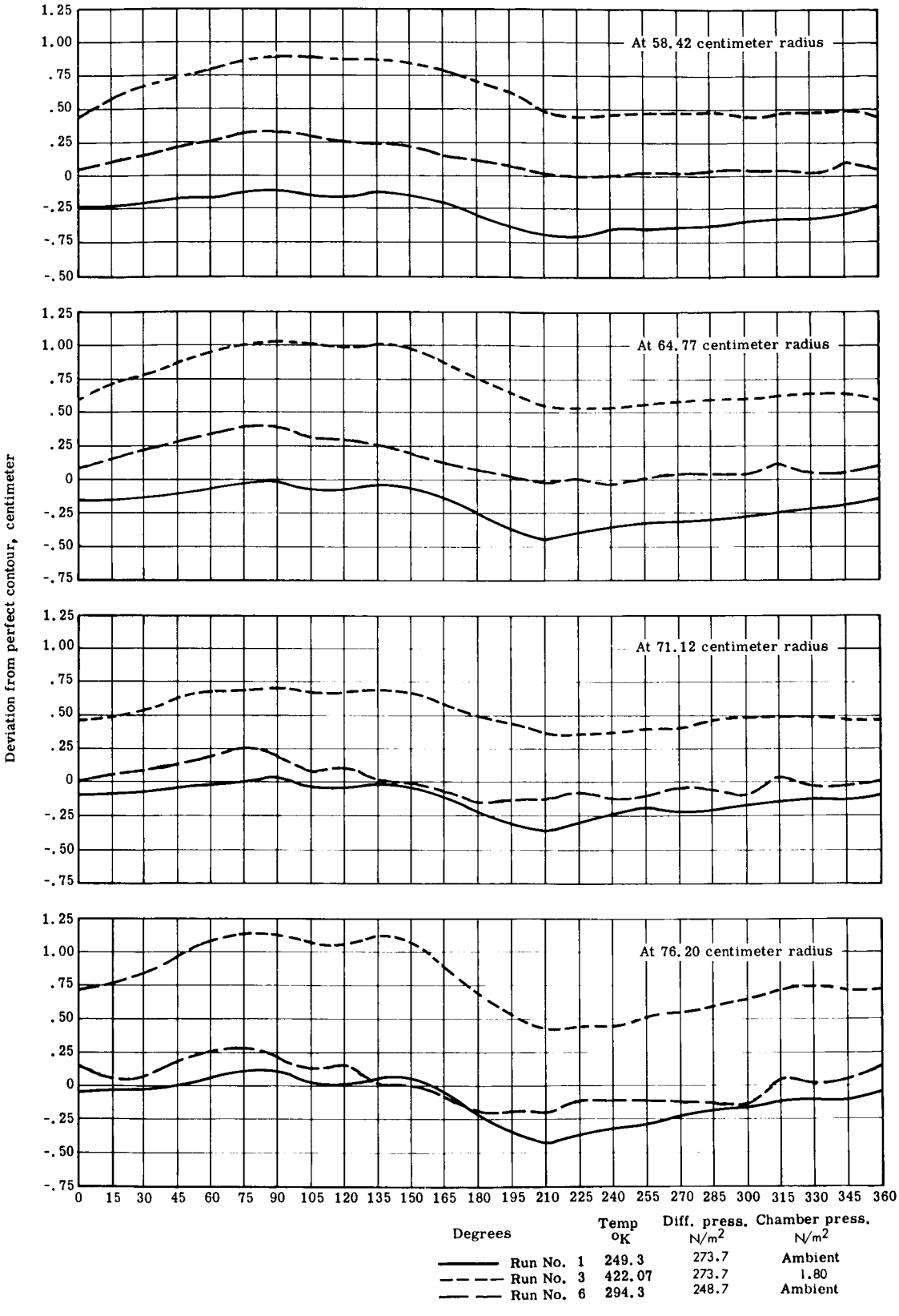

Figure 31 (Sheet 2). - Contour comparisons from all stations before, during, and after application of backup structure - final mirror.

to set the parabolic shape with the focal point retracted initially in order to obtain a final contour approaching that of a true parabola.

Surface quality. - To evaluate the reflective surface of the concentrator, specular reflectance measurements were performed on a sample of the aluminized Kapton film and integrated over the solar spectrum. From the visual appearance of the material, it was assumed that these values would be low. The material was highly stretched, wrinkled in places, and semi-transparent.

Measurements were made at Minneapolis Honeywell Research Center on their integrated hemispherical reflectometer. The measurements were made on a 10 x 10 cm sample of the aluminized polyimide film randomly selected from the roll that the concentrators were made from. It should be noted that these tests were made only on the aluminized film with no foam backing.

Table XII gives the solar reflectance at 20 selected wavelengths for this sample.

Table XII. - Total solar reflectance for aluminized polyimide film,

Number	Wavelength (Meters)	Reflectance
1	337 x 10^{-9}	0.86
2	339 x 10^{-9}	0.88
3	441 x 10^{-9}	0.87
4	474 x 10^{-9}	0.88
5	506 x 10^{-9}	0.89
6	540 x 10^{-9}	0.89
7	575 x 10^{-9}	0.88
8	613 x 10^{-9}	0.89
9	653 x 10^{-9}	0.84
10	698 x 10^{-9}	0.84
11	748 x 10^{-9}	0.82
12	805 x 10^{-9}	0.85
13	871 x 10^{-9}	0.84
14	949 x 10^{-9}	0.87
15	042 x 10^{-9}	0.88
16	153 x 10^{-9}	0.87
17	296 x 10^{-9}	0.89
18	501 x 10^{-9}	0.89
19	851 x 10^{-9}	0.92
20	789 x 10^{-9}	0.92

The average of this total solar reflectance is 0.873. The diffuse reflectance for this sample was determined to be between 0.033 and 0.067 or an average of 0.050. This diffuse reflection was determined by use

of the laser diffuser device. This laser device used a wavelength of 1628×10^{-10} m.

By taking the diffuse reflectance from the total solar reflectance we obtain a specular reflectance of 0.823. These results indicate that aluminized polyimide film being used for these reflectors is about average from the standpoint of specular reflection and not of a lower value as anticipated.

The aluminized polyimide film appeared to be somewhat transparent. In order to evaluate this, additional tests were run to check light transmission. The results of these tests are shown in Table XIII.

Table XIII. - Aluminized film transparency test.

Wavelength (Meters)	Transmission
4×10^{-7}	0.001
8×10^{-7}	0.002
9×10^{-7}	0.006
12×10^{-7}	0.005
14×10^{-7}	0.002
16×10^{-7}	0.002
20×10^{-7}	0.002

The results of this transmission test indicates that the aluminized film in reality is quite opaque and not transparent as previously thought.

From this information, it can be seen that the material used for these reflectors is of average quality.

CONCLUSIONS AND RECOMMENDATIONS

The three goals set forth in the development program work statement were satisfactorily accomplished. No new major problem areas were encountered. These goals were:

(1) Rigidization material and process studies.

(2) Aluminized polyimide film seam development.

(3) Fabrication of a 1.52-meter diameter solar concentrator.

The first two of the above tasks were for the purpose of developing materials and techniques to a level which would permit confident accomplishment of the major goal of producing an acceptable 1.52-meter diameter parabolic solar concentrator in a simulated space vacuum environment.

This program was a second phase of an azide foam rigidizing system carried out previously by GAC for NASA-Langley. (Report No. CR 235, Development of a Predistributed Azide Base Polyurethane Foam for Rigidization of Solar Concentrators in Space.)

In scaling up production of prepolymer and in mixing and sheeting of precoat, the transition was made without difficulty from laboratory to conventional chemical engineering pilot plant procedures and equivalent results were obtained.

Suitable recrystallization procedures were found for additional purification of Structure X azide.

Thin layer chromatography and ultraviolet spectrophotometry were established as additional criteria of azide purity.

The precoat material may be processed into thin sheets and applied to a structure-like tile without distrubing its foam-rigidizing character.

A suitable adhesive material was selected, and spray techniques developed for making high quality seams in aluminized polyimide film. These seams required elevated temperature resistance.

A good quality 1.52-meter diameter solar concentrator was produced in the NASA-Langley 18.29 m vacuum sphere. This final demonstration model, and the preliminary unit, confirmed the following:

Operability of the foaming process at pressures in the 0.133 N/m^2

Reproducibility of the foaming process and the physical structure and quality of the mirror.

The following recommendations are submitted for future consideration:

(1) The development of a system for packaging and deploying a paraboloidal shape coated with precoat material.

(2) The actual deployment testing of either a spherical or lenticular unit containing the paraboloidal contour and including the actual rigidization of this shape in a vacuum.

(3) Solar concentrators of larger sizes (3.04-meter diameter or greater) may be foam rigidized in vacuum.

DISTRIBUTION LIST

Copies	
	NASA Langley Research Center Langley Station Hampton, Virginia 23365
1	Contracting Officer
15	Marvin D. Rhodes, Mail Stop 188B
1	Library, Mail Stop 185
1	R. L. Zavasky, Mail Stop 117
1	NASA Ames Research Center Moffett Field, California 94035 Attention: Library
1	NASA Flight Research Center P. O. Box 273 Edwards, California 93523 Attention: Library
	NASA Goddard Space Flight Center Greenbelt, Maryland 20771
1	Library
1	Luther W. Slifer, Jr.
	Jet Propulsion Laboratory 4800 Oak Grove Drive Pasadena, California 91103
1	Library
1	G. E. Sweetnam
1	Peter Rouklove
	NASA Manned Spacecraft Center Houston, Texas 77001
1	Library
1	Richard B. Ferguson

Copies	
	NASA Marshall Space Flight Center Huntsville, Alabama 35812
1	Library
1	Ernst Stuhlinger
1	NASA Western Operations 150 Pico Boulevard Santa Monica, California 90406 Attention: Library
1	NASA Wallops Station Wallops Island, Virginia 23337 Attention: Library
1	NASA Electronics Research Center 575 Technology Square Cambridge, Massachusetts 02139 Attention: Library
	NASA Lewis Research Center 2100 Brookpark Road Cleveland, Ohio 44135
1	Mail Stop 3-7
2	Robert L. Cummings
1	NASA John F. Kennedy Space Center Kennedy Space Center, Florida 32899 Attention: Code ATS-132
1	NASA Michoud Assembly Facility P. O. Box 26078 New Orleans, Louisiana 70126 Attention: Mr. Henry Quintin, Code I-Mich-D

DISTRIBUTION LIST

Copies

Headquarters, NASA
Washington, D. C. 20546

1 Library, Code USS-10

1 Preston T. Maxwell, Code RNW

1 James R. Miles, Code SL

1 A. M. Andrus, Code ST-2

Air Force Aeropropulsion Laboratory
Research And Technology Division
Wright-Patterson AFB, Ohio 45433

1 Lt. I. R. Thompson (APIP-1)

1 Al Wallis (APIP-2)

1 Chief, Naval Bureau of Weapons
Department of the Navy
Washington, D. C. 20360
Attention: RAPP-14

1 U. S. Army Signal R&D Laboratory
Power Sources Division
Fort Monmouth, New Jersey 07703
Attention: Richard Nichols

1 University of Pennsylvania
Power Information Center
Moore School Building
200 South 33rd Street
Philadelphia, Pennsylvania 19104

54 Plus Re-pro-ducible National Scientific and Technical Information Facility
P. O. Box 33
College Park, Maryland 20740